NJC

Aqueous Solubilization of Hydrophobic Tetrapyrrole Macrocycles by Attachment to an Amphiphilic Single-Chain Nanoparticle (SCNP)

Journal:	*New Journal of Chemistry*
Manuscript ID	NJ-ART-09-2020-004413.R1
Article Type:	Paper
Date Submitted by the Author:	28-Oct-2020
Complete List of Authors:	Liu, Rui; North Carolina State University, Department of Chemistry Liu, Sijia; North Carolina State University, Chemistry Hu, Gongfang; North Carolina State University, Department of Chemistry Lindsey, Jonathan; North Carolina State University, Chemistry

Aqueous Solubilization of Hydrophobic Tetrapyrrole Macrocycles by Attachment to an Amphiphilic Single-Chain Nanoparticle (SCNP)

Rui Liu,[a] Sijia Liu,[a] Gongfang Hu, and Jonathan S. Lindsey*

[a]Equal contributions by both authors.

Department of Chemistry, North Carolina State University, Raleigh, North Carolina 27695-8204

Email: jlindsey@ncsu.edu

Abstract

Solubilization of hydrophobic tetrapyrrole macrocycles and other fluorophores in aqueous solution has been achieved by covalent attachment to the terminus of an amphiphilic polymer, thereby affording a single-fluorophore–single-chain nanoparticle (SCNP). The polymer is a heterotelechelic random polyacrylate/polyacrylamide copolymer bearing hydrophobic and hydrophilic pendant groups. The polymer has a folded unimeric morphology (~13 nm hydrodynamic diameter) in 1 M NaCl aqueous solution as indicated by dynamic light-scattering spectroscopy. Five hydrophobic organic fluorophores (coumarin, perylene, two chlorins, one phthalocyanine) have been synthesized with a conjugatable tether. Covalent conjugation of the fluorophore–maleimide to the polymer terminus via thiol–maleimide reaction was carried out in DMF. The resulting fluorophore–SCNP in 1 M NaCl aqueous solution exhibited retained spectral features and fluorescence quantum yield comparable to those of the respective hydrophobic benchmark in toluene. This single-fluorophore–single-polymer strategy simplifies the challenging and often idiosyncratic syntheses of water-soluble tetrapyrrole macrocycles by using the polymer as a general aqueous solubilization package, and in so doing opens up opportunities for the application of hydrophobic fluorophores in the life sciences.

Introduction

The emergence of synthetic dyes in the mid-19th century led quickly to recognition of the problem of dye aggregation, which occurs in organic solution but is most pronounced in aqueous solution, where many desirable applications reside. Simple manifestations of dye aggregation include metachromasy[1] (i.e., change in color with altered environment, including a change of concentration) and quenching of fluorescence.[2] A scientific objective that dye aggregation often stymies is the pursuit of high brightness. Intuitively, brightness refers to the extent of detected emission following absorption of a given sample.[3] A common strategy to increase fluorescence brightness is to increase the number of dyes per sample; in other words, increase the local dye concentration. Yet this approach often is only valid over a limited range of concentration owing to static and/or dynamic quenching of one dye by another.

The vast majority of dyes bear intrinsic charge as part of the conjugated π-system that constitutes the chromophore.[4] The presence of intrinsic charge typically facilitates solubilization in aqueous media, as exemplified by bioconjugatable cyanine dyes,[5] but alone may not preclude dye–dye aggregation. On the other hand, a number of chromophores (e.g., carotenoids, perylenes, quinones, tetrapyrroles) lack intrinsic charges,[4] and for these systems the challenge of aqueous solubilization is acute. A typical solution is to create a 3-dimensional superstructure that envelops the hydrophobic chromophore while presenting a hydrophilic exterior to the aqueous environment. One epitome of a fine-chemical molecular superstructure is provided by the phthalocyanine termed **La Jolla Blue** (Chart 1), first reported in the clinical chemistry literature in 1993[6] as well as in a patent[7] later in the decade. The molecular design employs long PEG chains disposed on opposite faces of the phthalocyanine macrocycle via attachment to a centrally ligated silicon atom, and bioconjugatable carboxylic acid groups attached to one of the peripheral benzo substituents. Other variants have been described wherein a sulfonate is attached to one of the benzo substituents

thereby enhancing water solubility.[8] Facial encumbrance has proved to be a generally viable design motif for imparting water solubility to diverse tetrapyrrole macrocycles[9] (e.g., porphyrins such as **FbP**;[10] chlorins such as **FbC** and **ZnC**;[11,12] and bacteriochlorins[13]) yet the chemical synthesis in almost all cases remains lengthy and generally requires manipulations of the intact macrocycle. The latter transformations often proceed in modest yield. Phthalocyanines in particular have been little employed in the life sciences owing to the challenges associated with aqueous solubilization. Still, tetrapyrrole macrocycles remain of great interest given their photoactivity and wavelength tunability in the red and near-infrared regions of the spectrum.[3]

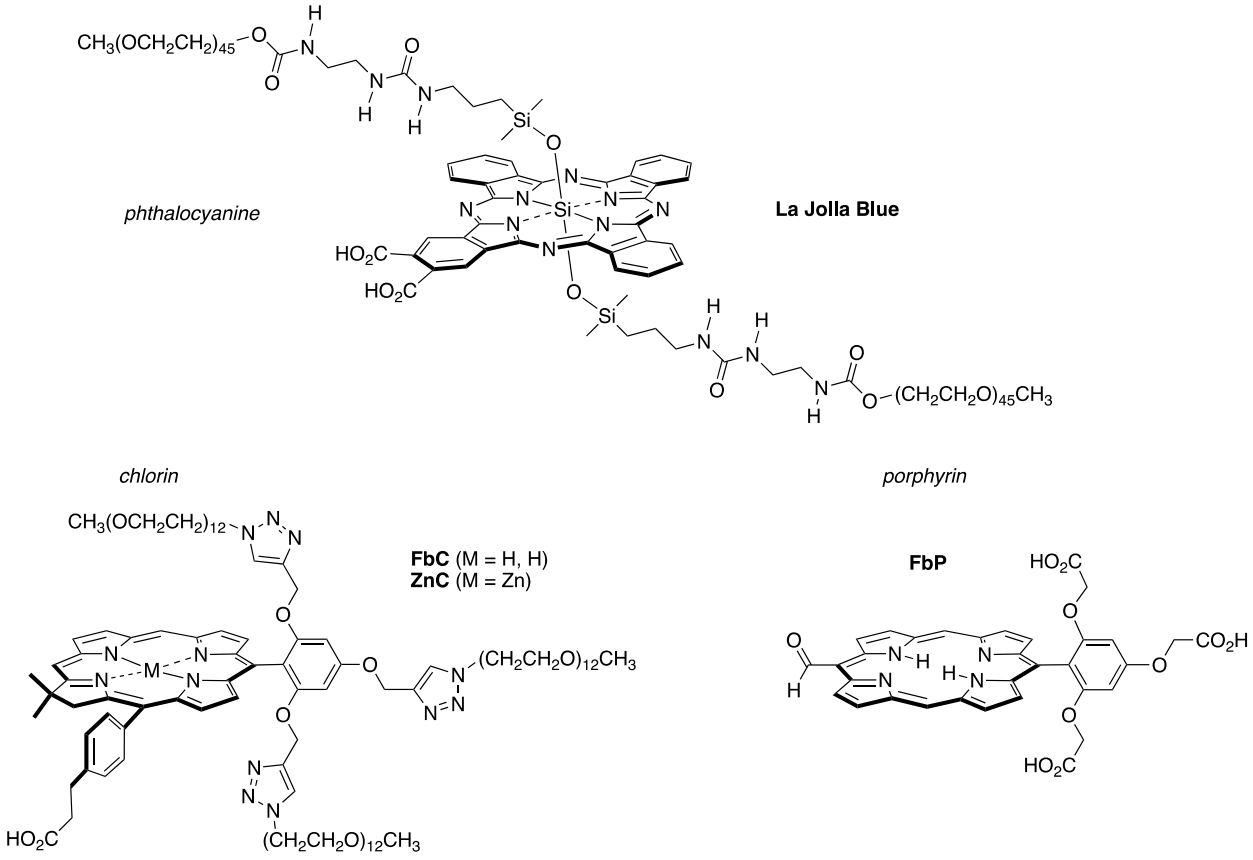

Chart 1. Water-soluble bioconjugatable tetrapyrroles. A phthalocyanine (top),[6,7] two chlorins (left bottom),[12] and a porphyrin (right bottom).[10] In the chlorins and porphyrin, the meso-aryl substituent orientation is largely perpendicular to the plane of the macrocycle, as illustrated.

New molecular designs in the ensuing quarter century have relied on broadly defined "nanoparticles" to assemble dyes for use in aqueous solution. A particularly attractive approach in our eyes was the use of single-chain nanoparticles (SCNPs), where each SCNP is composed of an amphiphilic polymer. The amphiphilic polymer in aqueous solution undergoes "single-chain collapse" thereby creating a hydrophobic interior and hydrophilic exterior. Hydrophobic dyes attached to the polymer can thus be enveloped in the protective cocoon of the interior hydrophobic region of the folded polymer. Numerous polymer compositions, polymerization methods, and dye attachment strategies have been described, as have designs for side-chain cross-linking and derivatization. This topic has been extensively studied over the past decade.[14-23]

A general approach to achieve increased brightness has been to attach numerous dyes as pendant groups to the polymer that gives the SCNP.[14-16,18-20,24,25] We have moved in the opposite direction, to attach a single dye (hereafter termed a fluorophore) to the SCNP. The impetus for doing so is to avoid any possibility for fluorophore–fluorophore quenching upon intramolecular folding. To reliably attach a single fluorophore without statistical distribution, we have attached the fluorophore at one terminus of the polymer, and for maximum design versatility, we have employed post-synthesis modification of a heterotelechelic polymer. In this strategy, the synthesis of a hydrophobic fluorophore and the synthesis of the solubilization package (the amphiphilic polymer) are separated into different spheres of activity. The resulting single-cargo–single-polymer design contains the hydrophobic fluorophore at one terminus of the polymer and a bioconjugatable group at the other terminus. The single-fluorophore–single-polymer design has been examined previously by others (see Discussion); the advances reported here concern the amenability toward incorporation of diverse hydrophobic fluorophores (including tetrapyrrole macrocycles) and the retention of fluorescence brightness of the construct in aqueous solution.

The specific molecular architectures employed were inspired by the work of the research groups of Sawamoto and Kamachi.[26-29] After a period of exploration, the general synthetic route that we settled on for preparing the polymer and fluorophore–polymer conjugates is shown in Scheme 1.[30] Polymerization via radical atom fragment transfer (RAFT)[31-35] of three monomers with a chain transfer reagent affords the corresponding heterotelechelic amphiphilic polymer. Preparation of the polymers and fluorophore–polymer conjugates can be carried out in one week beginning with monomers and suitably conjugatable fluorophores. Each polymer contains two distinct functional groups on each end of the backbone for conjugation: (1) reaction of **F-Ph** with a primary amine reveals the terminal thiol (**F-SH**) by cleavage of the dithiobenzoate, enabling *in situ* conjugation with a fluorophore–maleimide; (2) reaction of the thiol of **F-SH** with *p*-bromomethylbenzaldehyde affords **F-CHO**, enabling reaction with a hydrazide-containing fluorophore to form a hydrazone. The purification of the fluorophore–polymer conjugate from free fluorophore is carried out by dialysis in *N,N*-dimethylformamide (DMF), where the polymer is regarded as largely unfolded. On the other end of the polymer backbone, all three polymers (**F-Ph**, **F-SH**, and **F-CHO**) bear a carboxylic acid, derived from the chain transfer agent, which opens the possibility of attachment to specific targets (proteins, antibodies, second fluorophores, surfaces, etc.).

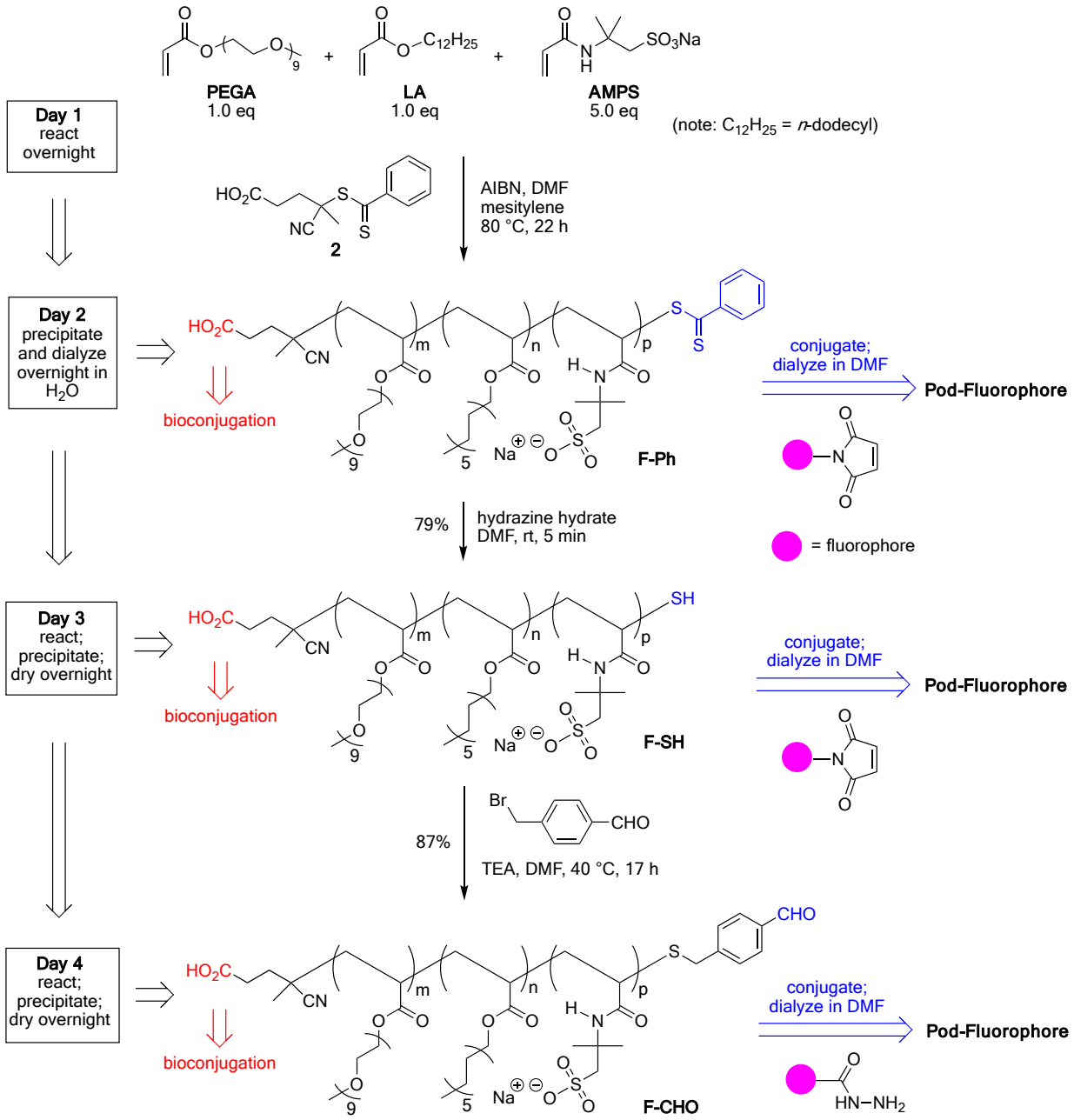

Scheme 1. Flow chart of the polymer synthesis and derivatization.†

We explored the single-cargo–single-polymer† approach using 8 classes of conjugatable fluorophores and reported the results in a communication.[30] The fluorophore classes encompass a coumarin (λ_{em} 482 nm), BDPY (λ_{em} 512 nm), rhodamine (λ_{em} ~564 nm), Cy3-cyanine (λ_{em} 570 nm), perylene-monoimide (λ_{em} 573 nm), chlorin (λ_{em} 641 nm), zinc phthalocyanine (λ_{em} 696 nm),

and bacteriochlorin (λ_{em} 765 nm). A second study concerned morphological changes and fluorescence readout upon metal chelation-induced dimerization of a dipyrrinato-conjugated SCNP.[36] The conjugatable fluorophores (except the phthalocyanine) are shown in Chart 2. In this paper, we describe an expansion of the fluorophore–SCNP approach. In part 1, the syntheses of three prior (**PMI-mal**, **Chl-hydrazide**, and **coumarin-hydrazide**) and two new conjugatable fluorophores are described (the other four prior examples in Chart 2 were commercially available or known compounds,[37] and the dipyrrin has been described[36]). In part 2, the polymer **F-Ph** is characterized by a variety of techniques. In part 3, two new fluorophore–SCNPs are described where the fluorophore is a free base chlorin or a zinc phthalocyanine. Taken together, the work describes a simple strategy for encapsulation of hydrophobic fluorophores with retention of fluorescence brightness in aqueous solution.

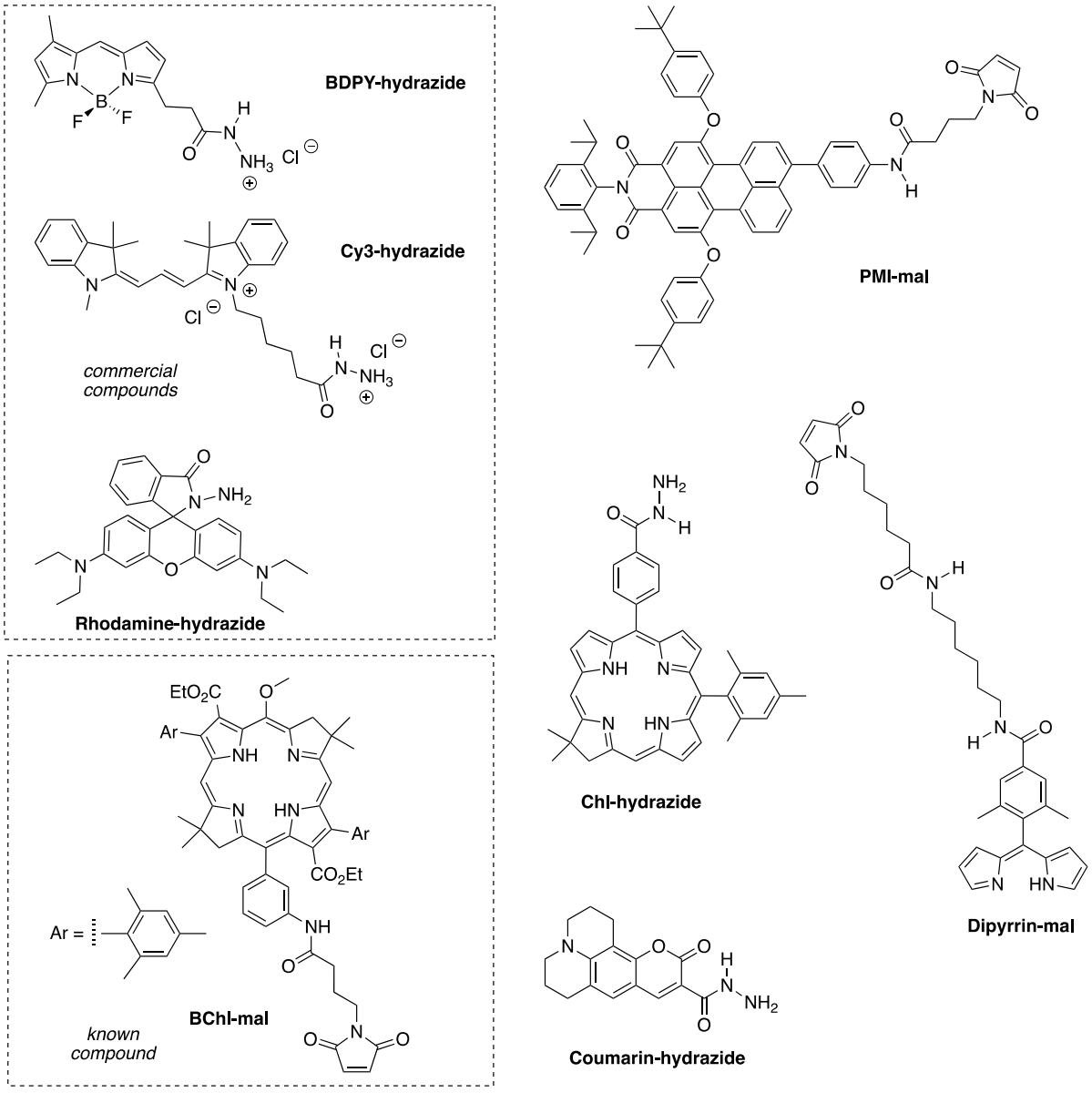

Chart 2. Conjugatable fluorophores examined previously.

Results

1. Synthesis of Five Conjugatable Fluorophores.

The synthesis of **Coumarin-hydrazide** was carried out using a reported method[38] (Scheme 2). **Coumarin 314** bearing an ethyl ester in ethanol was treated with excess hydrazine hydrate to give the corresponding **Coumarin-hydrazide** in 63% yield. Reaction of **Coumarin-hydrazide** with *p*-tolualdehyde gave the **Coumarin-hydrazone** in 94% yield. Iodochlorin **1**[39] was

quantitatively transformed into the methyl ester **2** by reaction with $Pd(PPh_3)_4$, methanol and carbon monoxide (Scheme 2). Treatment of **2** with hydrazine hydrate under reflux generated the desired chlorin **Chl-hydrazide** in 83% yield. The reaction was carried out at a concentration below 50 mM, because higher concentrations resulted in the reduction of chlorin to the corresponding bacteriochlorin as evidenced by absorption spectroscopy. When the bacteriochlorin was observed, oxidation with DDQ afforded the **Chl-hydrazide**. Regardless, **Chl-hydrazide** slowly decomposed in solution as evidenced by ^{1}H NMR spectroscopy. For these reasons as well as incomplete reaction with the polymer (*vide infra*), we explored a conjugatable linker that features a maleimide moiety for thiol–maleimide coupling.

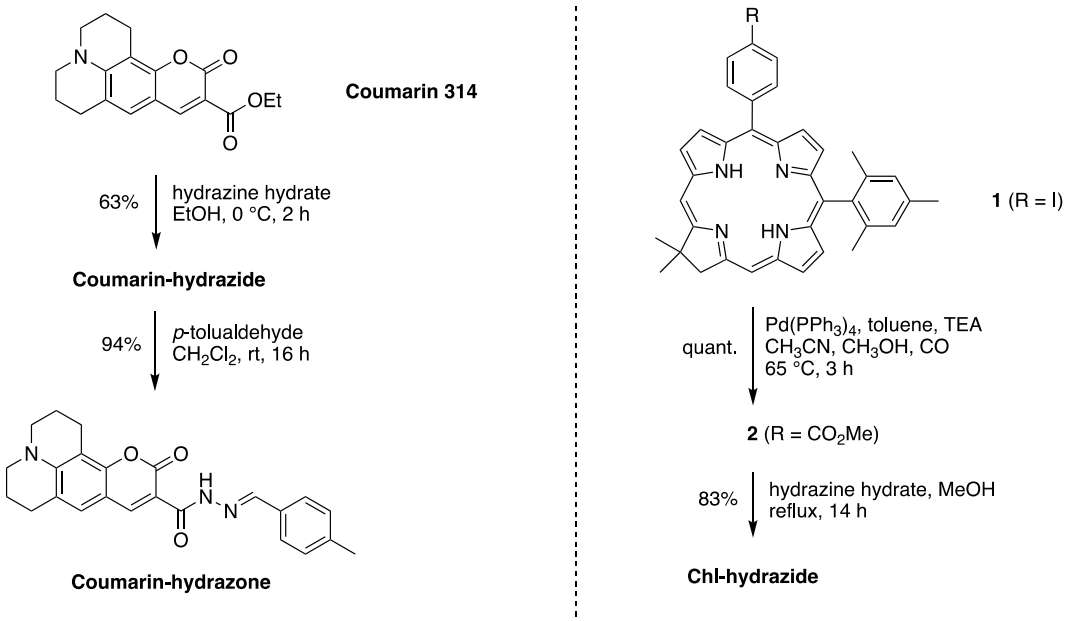

Scheme 2. Synthesis of fluorophore–hydrazides.

The installation of a maleimide group to a chlorin and a perylene-monoimide is shown in Scheme 3. Free base bromochlorin **Chl-Br**[40] was reacted with 4-aminophenylboronic acid pinacol ester **3** via Suzuki coupling[39] to give the corresponding aminochlorin **Chl-NH$_2$**[40] in 47% yield (Scheme 3). Coupling with 4-(*N*-maleimido)butyric acid (**Mal-acid**) in the presence of the condensation agent 1-ethyl-3-(3-dimethylaminopropyl)carbodiimide hydrochloride (EDC)[41] gave

the chlorin–maleimide **Chl-mal** in 44% yield. Palladium-mediated Suzuki coupling[42] of **PMI-Br**[43] and **3** in toluene gave the aminoperylene **PMI-NH$_2$** in 43% yield. EDC coupling[41] of **PMI-NH$_2$** and **Mal-acid** in dichloromethane gave the perylene–maleimide **PMI-mal** in 76% yield.

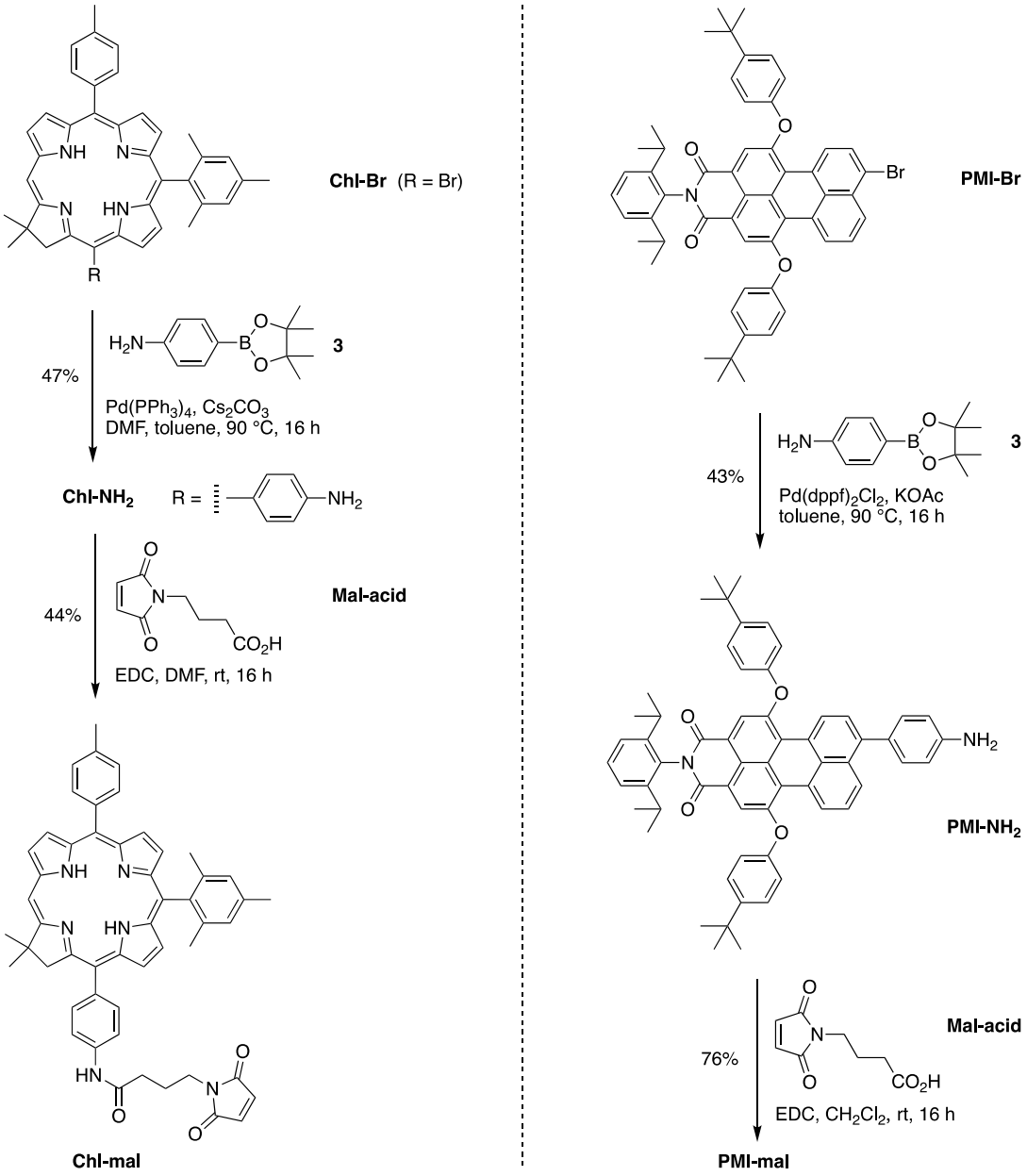

Scheme 3. Synthesis of fluorophore–maleimides.

The synthesis of the zinc phthalocyanine–maleimide **ZnPc(*t*-Bu)$_3$-mal** is shown in Scheme 4. Known[44] amino-substituted zinc phthalocyanine **ZnPc(*t*-Bu)$_3$-NH$_2$**, which exists as a mixture

of positional isomers, was coupled with **Mal-acid** in the presence of *N,N*-dicyclohexylcarbodiimide (DCC) to afford the corresponding **ZnPc(*t*-Bu)$_3$-mal** in 40% yield (Scheme 4). Limited solubility and aggregation even in coordinating solvents (pyridine-d_5, THF-d_8) precluded collection of satisfactory ^{1}H and ^{13}C NMR spectra. The conjugatable phthalocyanine could not be characterized to the full standards expected in organic chemistry research, although the mass analysis was accurate.

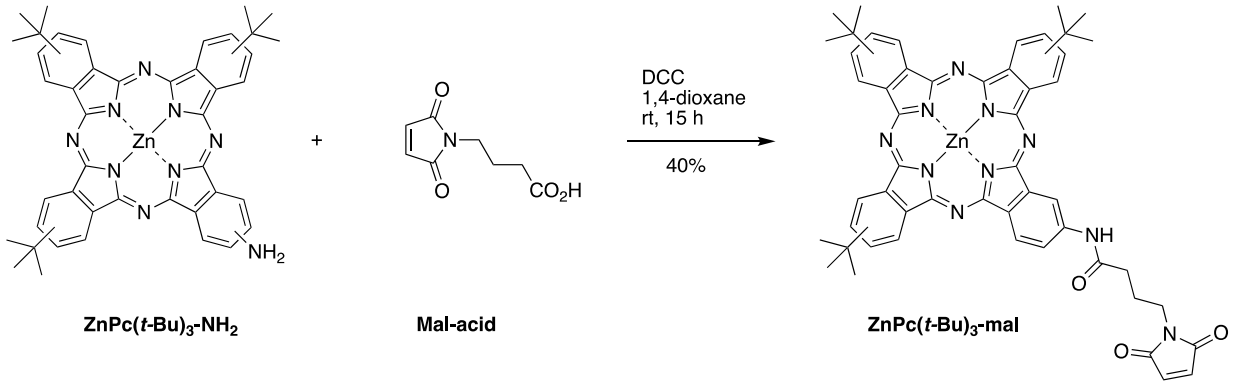

Scheme 4. Synthesis of a phthalocyanine–maleimide.

2. Synthesis and Characterization of Amphiphilic Polymer F-Ph.

The polymer **F-Ph** was previously prepared by RAFT polymerization of a polyethylene glycol derivatized acrylate (**PEGA**), lauryl acrylate (**LA**), and a sulfonate derivatized acrylamide (**AMPS**) in 1:1:5 ratio followed by workup, which entailed precipitation and dialysis as outlined in Scheme 1.[30] Here, we prepared a second batch of **F-Ph** and carried out characterization by absorption spectroscopy, ^{1}H NMR analysis, analytical size-exclusion chromatography (SEC), and dynamic light-scattering (DLS) spectroscopy (Figures S1-S4). The key findings are as follows: (1) the molecular composition of the polymer was nearly identical to that of the initial 1:1:5 ratio of monomers (by ^{1}H NMR spectroscopy); (2) the M_n was 36 kDa with a polydispersity index (PDI, $Đ = M_w/M_n$) value of 1.55 (by analytical SEC in DMF), corresponding to m, n, and p = 18, 18, and 90, respectively; (3) the hydrodynamic radius (D_h) in 1 M NaCl aqueous solution was ~13 nm (by

DLS analysis); and (4) absorption spectroscopy showed the characteristic band of the dithiobenzoate group at 305 nm. The PDI is consistent whereas the M_n is slightly lower (36 kDa) than those values for the previous batch of **F-Ph** (40 kDa), which exhibited m, n, p = 20, 20, 100, respectively.[30] The data for this second batch of **F-Ph**, which illustrate the general repeatability of the polymer synthesis, are shown in the Supplementary Information.

3. Synthesis and Characterization of Fluorophore–SCNPs.

Conjugation of a fluorophore and the polymer was achieved previously via an aldehyde–hydrazide or thiol–maleimide joining reaction.[30] The aldehyde–hydrazide route afforded incomplete reaction and consequent low fluorophore loading ratios on the polymers. In contrast, the thiol–maleimide chemistry exhibits several advantages: (1) high efficiency under very mild conditions and low concentration; (2) more facile synthesis of a fluorophore bearing a maleimide versus hydrazide linker; and (3) diminished synthetic manipulation of the polymer because **F-Ph** can be converted *in situ* to **F-SH** and the latter reacted with a fluorophore–maleimide in excess. Here, a fluorophore–maleimide (**Chl-mal**, **ZnPc(*t*-Bu)$_3$-mal**) was reacted with **F-Ph** in DMF containing ethanolamine at room temperature for 16 h followed by dialysis in DMF for 24 h to remove excess fluorophore (Scheme 5). The dialysis process in DMF enables free fluorophore to be removed from the much higher molecular weight fluorophore–polymer conjugate. The dialyzed solution was dried under high vacuum. The resulting solid was dissolved in water and lyophilized overnight to afford the fluorophore–SCNP termed† **Pod-Chl** or **Pod-ZnPc(*t*-Bu)$_3$**. **Pod-Chl** and **Pod-ZnPc(*t*-Bu)$_3$** were prepared from the first and second batches of **F-Ph**, respectively, which are almost identical in size and composition (*vide supra*).

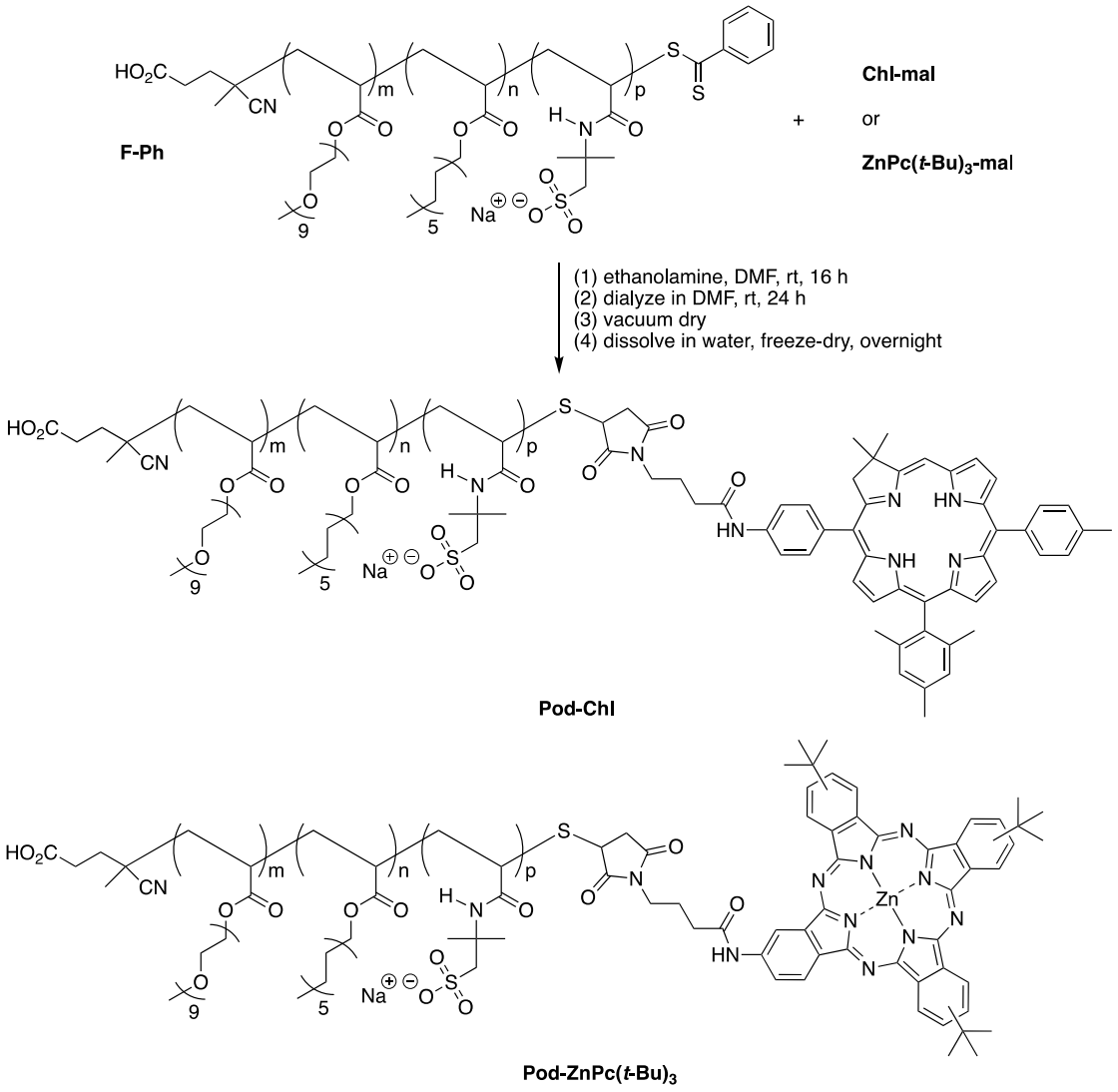

Scheme 5. Synthesis of two new fluorophore–Pods, also termed fluorophore–SCNPs.†

The spectral features and properties of **Pod-Chl** or **Pod-ZnPc(*t*-Bu)$_3$** were compared with two benchmark compounds, the chlorin **Chl-TM** (TM = *p*-tolyl and mesityl) and the phthalocyanine **ZnPc(*t*-Bu)$_4$** (Chart 3). The fluorophore–Pods were examined in 1 M NaCl aqueous solution whereas the benchmark compounds were examined in organic solvents. The **Pod-Chl** was further compared with chlorin–polymer conjugate, **Pod-Chl-hydrazone**, wherein the chlorin is linked to the polymer via a hydrazone. The perylene-monoimide conjugated polymer, **Pod-PMI**, provided for further comparisons (*vide infra*).

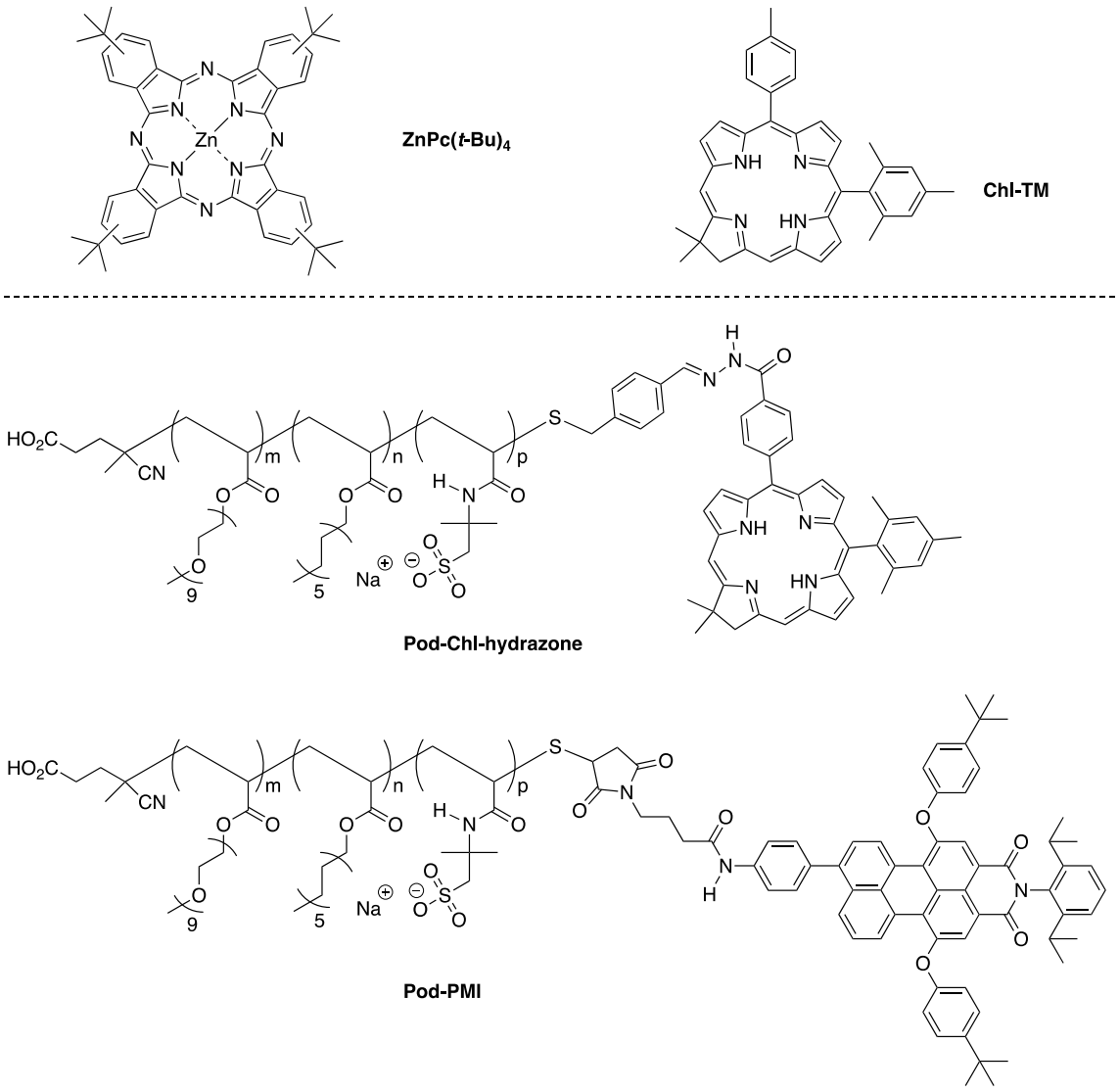

Chart 3. Fluorophore benchmarks and previously reported fluorophore–Pods.

The absorption and fluorescence spectra of **Pod-Chl** and **Pod-Chl-hydrazone** are shown in Figure 1 along with those of the benchmark **Chl-TM** (<10 μM of each). The **Pod-Chl-hydrazone** in 1 M NaCl aqueous solution exhibits absorption spectral features that closely resemble those of the benchmark chlorin **Chl-TM** in toluene. The intense B band (~400 nm) and the Q_y band (641 nm) for **Pod-Chl-hydrazone** are nearly identical with those of **Chl-TM** despite the different media. The fluorescence emission band in each case was located at 646 nm. The value for the fluorescence quantum yield (Φ_f) was 0.19 for **Pod-Chl-hydrazone** in 1 M NaCl

aqueous solution versus 0.22 for **Chl-TM** in toluene, indicating a high degree of retention of spectral features and fluorescence intensity.

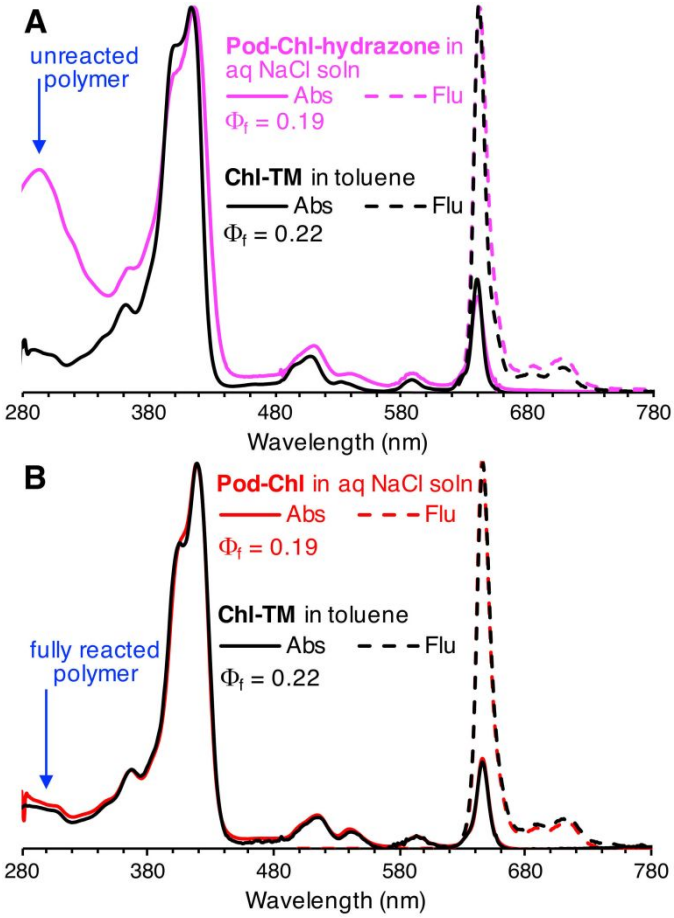

Figure 1. Absorption and fluorescence spectra at room temperature of (A) **Pod-Chl-hydrazone** and (B) **Pod-Chl** (containing a thiol–maleimide linker). The fluorophore–Pods are in aqueous solution containing 1 M NaCl whereas the chlorin benchmark **Chl-TM** is in toluene.

On the other hand, the absorption spectrum of **Pod-Chl-hydrazone** showed a large band at ~293 nm that was not present in **Chl-TM**.[30] The absorption is attributed to the presence of unreacted polymer **F-CHO** upon formation of the hydrazone. On the basis of the molar absorption coefficients for **Chl-TM** (main visible band 89,100 $M^{-1}cm^{-1}$),[45] a hydrazone benchmark ($\varepsilon_{280\ nm}$ = 13,200 $M^{-1}cm^{-1}$),[46] and **F-CHO** ($\varepsilon_{308\ nm}$ = 6,800 $M^{-1}cm^{-1}$), the mixture is composed of **Pod-Chl** (30%) and **F-CHO** (70%). The presence of the unreacted polymer **F-CHO** highlights a generic

limitation of the present approach – although excess fluorophore is readily removed by dialysis, purification of the fluorophore–polymer construct from the unreacted polymer is quite difficult. Moreover, the similarity of the Φ_f values for the **Pod-Chl-hydrazone** in 1 M NaCl aqueous solution and the benchmark chlorin **Chl-TM** (Chart 3) in toluene can be misleading in the context of brightness, because Φ_f is defined as the ratio of photons emitted to photons absorbed, whereas brightness concerns the number of photons emitted per a given quantity of absorbing sample. To achieve high brightness requires high efficiency conjugation protocols, where every polymer in the sample contains an attached fluorophore. In this regard, the spectral features of the **Pod-Chl** containing a thiol–maleimide linker are shown in Figure 1B. The absorption spectrum of the **Pod-Chl** in 1 M NaCl aqueous solution lacks the 290 nm peak, and is essentially identical to that of the benchmark **Chl-TM** in toluene in the wavelength region from 280–680 nm. Loading of the chlorin via the thiol–maleimide linker appears to be quantitative.

The **Pod-ZnPc(*t*-Bu)$_3$** exhibited absorption and fluorescence spectra (peak position, full-width-at-half-maximum, fwhm, Stokes shift) in 1 M NaCl aqueous solution that were almost identical (i.e., orthochromic) with those of **ZnPc(*t*-Bu)$_3$-mal** in toluene (<10 μM of each, Figure 2). Indeed, both **Pod-ZnPc(*t*-Bu)$_3$** and **ZnPc(*t*-Bu)$_3$-mal** exhibit a typically narrow Q_y absorption band (fwhm ~24 nm). The Φ_f value of **Pod-ZnPc(*t*-Bu)$_3$** in 1 M NaCl aqueous solution was 0.25, to be compared with 0.28 for **ZnPc(*t*-Bu)$_3$-mal** in toluene. The **Pod-ZnPc(*t*-Bu)$_3$** upon illumination in the ultraviolet gave a small amount of an unknown blue fluorescence that was not present in either **ZnPc(*t*-Bu)$_3$-mal** or **F-Ph** (Figure S5). We previously examined a phthalocyanine–Pod[30] where the phthalocyanine contained six heptyl groups.[47] While the characterization data for the maleimide-linked hexaheptylphthalocyanine were very limited, the corresponding phthalocyanine–Pod in 1 M NaCl aqueous solution exhibited a very broad Q_y absorption band (fwhm = 72 nm).[30] To the extent comparisons can be made given the limited

characterization data, the more compact tri-*tert*-butyl design (12 peripheral carbons) is superior to the hexa-*n*-heptyl architecture (42 peripheral carbons) in conjunction with the polymer **F-Ph**.

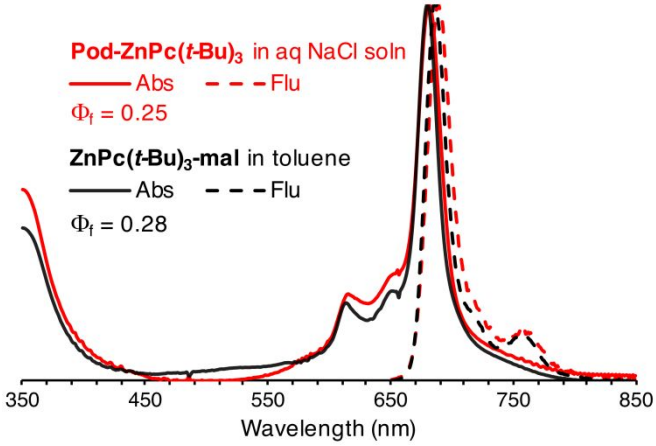

Figure 2. Absorption and fluorescence spectra at room temperature of **Pod-ZnPc(*t*-Bu)$_3$** (in 1 M NaCl aqueous solution) and benchmark **ZnPc(*t*-Bu)$_3$-mal** (in toluene).

The fluorophore–Pods where the fluorophore is a chlorin or zinc phthalocyanine could not be examined by DLS spectroscopy to assess the unimer composition. The limitation stems from coincidence of the strong absorption and fluorescence of chlorin and zinc phthalocyanine chromophores near 645 nm, and the DLS laser excitation at 633 nm. To examine a fluorophore–Pod by the full complement of DLS, absorption, and fluorescence spectroscopies, we turned to the use of a perylene-monoimide (PMI). The structure of the perylene-monoimide bearing a maleimide group (**PMI-mal**) is shown in Chart 2. The PMI chromophore has similar size to that of a tetrapyrrole macrocycle, yet absorbs and emits at 529 and 574 nm (in toluene), respectively (Figure 3A). The corresponding polymer bearing the attached perylene-monoimide, **Pod-PMI** (Chart 3), was prepared previously.[30]

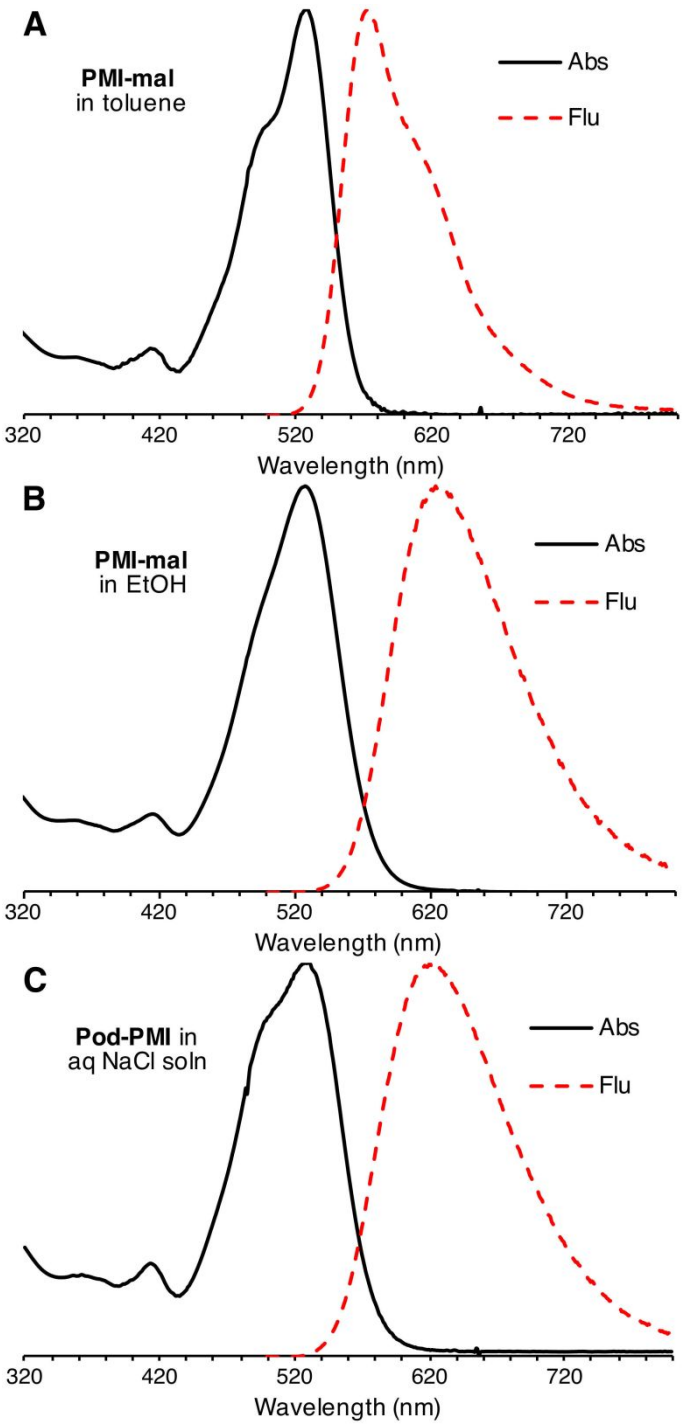

Figure 3. Absorption and fluorescence spectra at room temperature of **PMI-mal** in toluene (A), **PMI-mal** in EtOH (B) and **Pod-PMI** in 1 M NaCl aqueous solution (C).

The absorption and fluorescence spectra of **Pod-PMI** were examined in 1 M NaCl aqueous solution (Figure 3C). Both the absorption and fluorescence bands were slightly broadened versus

those of the hydrophobic benchmark **PMI-mal** in toluene. To understand the possible origin of the broadening, the spectra of **PMI-mal** were collected in mixtures of cyclohexane (CH) and ethanol, as well as in 100% ethanol (Figure S6, Table S1). **Pod-PMI** in 1 M NaCl aqueous solution displayed almost identical absorption and fluorescence spectra as **PMI-mal** in EtOH (Figure 3B). The data thus suggest that the local polarity encountered by the PMI unit in the **Pod-PMI** more closely resembles that of an aliphatic alcohol medium than that of toluene. The spectral data of the three fluorophore–Pods along with those for the benchmark compounds **Chl-TM** and **ZnPc(*t*-Bu)$_3$-mal** are summarized in Table 1.

Table 1. Spectral properties of three fluorophore–Pods in 1 M NaCl aqueous solution compared with their hydrophobic benchmarks in organic solvents.

Compounds	Solvent	λ_{abs} [fwhm] (nm)	λ_{exc} (nm)	λ_{em} [fwhm] (nm)	Φ_f
Pod-Chl	1 M aq NaCl	645 [12]	419	646 [13]	0.21[a]
Chl-TM	toluene	645 [12]	419	646 [12]	0.22[a]
Pod-ZnPc(*t*-Bu)$_3$	1 M aq NaCl	682 [25]	616	688 [24]	0.25[b]
ZnPc(*t*-Bu)$_3$-mal	toluene	680 [23]	612	685 [21]	0.28[b]
Pod-PMI	1 M aq NaCl	531 [86]	480	624 [104]	0.59[30]
PMI-mal	toluene	529 [69]	413	574 [77]	0.66[30]
PMI-mal	EtOH	528 [78]	413	624 [106]	0.41[c]

[a]Using **Chl-TM** in toluene (Φ_f = 0.22) as the standard.[48] [b]Using **ZnPc(*t*-Bu)$_4$** in toluene (Φ_f = 0.33) as the standard.[49] [c]Using **PMI-mal** in toluene (Φ_f = 0.66) as the standard.[30]

Finally, one control experiment was carried out to assess the importance of conjugation of the fluorophore to the polymer. Equimolar quantities of **ZnPc(*t*-Bu)$_4$** and **F-Ph** were dissolved in DMSO (0.1 mL) followed by the addition of 100 mL of 1 M NaCl aqueous solution. The major

absorption band was extremely broad (fwhm = 85 nm) and the fluorescence intensity was weak ($\Phi_f = 0.005$), to be compared with fwhm = 25 nm and $\Phi_f = 0.25$ for **Pod-ZnPc(*t*-Bu)$_3$** in 1 M NaCl aqueous solution. The stark contrast between the sharp absorption spectrum and retained fluorescence of **Pod-ZnPc(*t*-Bu)$_3$** versus that of the analogous unattached but non-covalently assembled system highlights the importance of conjugation to form the intact single-fluorophore–single polymer system.

Discussion

Modern approaches to thwart fluorophore aggregation rely on a variety of design features including adding charged groups to create electrostatic repulsion between fluorophores, adding steric bulk to block π–π interactions between fluorophores, and embedding fluorophores in protective environments. Such approaches often entail distinct designs for each type of fluorophore, with further idiosyncratic tailoring for each specific fluorophore. The work herein is aimed at developing a more general solution to the challenge of fluorophore solubilization, particularly for members of the tetrapyrrole family. The tetrapyrrole family includes porphyrins, chlorins, bacteriochlorins, and more expansively, the phthalocyanines, all of which contain a large aromatic macrocycle. The tetrapyrrole family provides wavelength tunability in the comparatively under-utilized red and near-infrared spectral region.[3]

The attachment of porphyrins to polymers dates most notably to the work of Kamogawa,[50] Kamachi,[51] and Tsuchida[52] and their respective groups nearly 50 years ago, although pioneering work with chlorin–polymers was reported by Lautsch[53,54] (a former associate of Hans Fischer) and coworkers a generation earlier. The impetus for such work was to achieve novel catalysts or receptors, thereby mimicking photosynthetic, enzymatic, and hemoglobin-like functions. The molecular designs generally entailed incorporation of the tetrapyrrole macrocycle as a pendant

group in a hydrophobic copolymer, although attachment to polyethyleneimine via an amide linkage also was explored. The work of Cellarius and Mauzerall wherein tetrapyrrole macrocycles were coated onto polystyrene nanoparticles to create a light-harvesting apparatus, while not a covalent architecture, also warrants comment in this regard.[55] The evolution of methods of polymerization in the ensuing years has made possible diverse new architectures for incorporation of hydrophobic macrocycles.

The single-cargo–single-polymer approach reported herein was inspired by the pioneering work of groups led by Sawamoto and by Kamachi. The Sawamoto group mainly focused on using various PEG groups as the hydrophile and various linear hydrocarbon chains as the hydrophobe group (via atom transfer radical polymerization, ATRP) on methacrylate monomers to achieve a unimer in water.[27-29] The Kamachi group used an acrylamide monomer that contains sulfonate (**AMPS**) as the hydrophile and created polymers via free radical polymerization, in some cases including a pendant fluorophore at a low percentage of incorporation.[26] After a period of exploration using **PEGA**, **LA** and **AMPS** in ATRP, we switched to RAFT and settled on the 1:1:5 ratio of monomers, respectively, leading to **F-Ph**.[30]

Derivatization of the end groups of polymers made by RAFT polymerization is well known, including orthogonal derivatization of heterotelechelic polymers.[56-58] The attached groups include a range of chromophores;[58] for representative examples, see references 59-76. Most cases where a cargo unit has been incorporated at an end group concern hydrophobic or hydrophilic polymers.[59-78] Few cases are known where a cargo entity has been incorporated at an end group of an amphiphilic polymer, and the resulting polymer–cargo construct has been demonstrated to undergo self-assembly in aqueous solution.[79-81] In such cases, the retention of fluorescent brightness was rarely if ever considered. A common approach to incorporate fluorophores to polymers has entailed attachment as pendant groups,[14,16] the rationale being that a large number of

fluorophores per polymer would support a high level of brightness. Our work here has focused on use of the polymer as an envelope to shelter a single fluorophore from other fluorophores and thereby retain high fluorescent brightness in aqueous solution. The use of one fluorophore per polymer avoids the statistical distribution of polymers bearing various numbers of fluorophores, and the accompanying problem of spectral variation and fluorescence quenching that varies across the distribution owing to juxtaposition of multiple fluorophores upon single-chain collapse of the polymer.

Brightness can be assessed in a number of ways.[3] An experimental measure of brightness (B_E) for molecules in solution is given by the product of the molar absorption coefficient (ε) at the wavelength of excitation and the fluorescence quantum yield (Φ_f). A further measure is given by the brightness per unit volume (B_E/V).[18] The values for **Pod-Chl** and **Pod-ZnPc(*t*-Bu)$_3$** are estimated in Table 2. Two points are noteworthy. First, as stated above, the Φ_f value of the fluorophore–SCNP constructs in aqueous solution is very similar to that of the fluorophore alone in toluene. (Assessments of the increase in brightness for the fluorophore in going from aqueous solution to a packaged environment have merit, but can be misconstrued because there is inevitably a large extent of quenching of the fluorophore alone in aqueous solution.) Second, the B_E/V values are rather low here (4.6, 34) due to the large size of the SCNP, which is taken to have V = 1.15 x 10^3 nm^3 (corresponding to a unimeric particle of 13 nm diameter). As a point of comparison, the value for rhodamine 101 is 166,000, although polymer nanoparticles loaded with multiple fluorophores typically have values in the few hundred to few thousand range. For many applications, it is not brightness per unit volume (B_E/V) that matters but brightness per particle (e.g., antibody, scaffold, cell), and the latter can be increased by attachment of multiple fluorophores to a given particle. The attachment of multiple copies of fluorophore–SCNPs to carrier scaffolds will be the subject of future investigation.

Table 2. Brightness considerations.

Fluorophore–Pod	ε ($M^{-1}cm^{-1}$)	Φ_f [c]	Brightness [d] (B_E, $M^{-1}cm^{-1}$)	B_E/V [e] ($M^{-1}cm^{-1}nm^{-3}$)
Pod-Chl	28,000[a]	0.19	5.3×10^3	4.6
Pod-ZnPc(*t*-Bu)$_3$	220,000[b]	0.176	3.9×10^4	34

[a]Value for **Chl-TM** from Ref 45. [b]Value for **ZnPc(*t*-Bu)$_4$** from Ref. 49. [c]Value for the fluorophore–Pod. [d]Brightness (B_E) is given by $\varepsilon \cdot \Phi_f$ (Fluorophore–Pod). [e]$V = 1.15 \times 10^3$ nm^3 for a unimeric particle of 13 nm diameter.

Conclusions.

The attachment of a hydrophobic fluorophore at one terminus of a suitably designed amphiphilic polymer affords a means of solubilization of the fluorophore in aqueous solution. The polymer employed herein (36 kDa) was prepared by RAFT polymerization and contains three types of pendant groups (PEG, lauryl and sulfonate in ~1:1:5 ratio) and distinct terminal groups (carboxylic acid, benzothioate). Attachment of a maleimido-substituted fluorophore to the thiol-terminated polymer is superior to the hydrazone linkage explored previously. The absorption and fluorescence spectral features (including the Φ_f values) of the fluorophore–SCNPs were examined in 1 M NaCl aqueous solution and found to be nearly identical to those of the corresponding benchmark fluorophores in toluene. The fluorophores of interest at present include those that absorb and emit in the red and near-infrared spectral regions, which have been less explored than shorter-wavelength spectral regions yet also are amenable to biomedical applications where deep tissue penetration of light is desired. The compact tri-*tert*-butylphthalocyanine in conjunction with the polymer employed herein was readily soluble in 1 M NaCl aqueous solution, providing a

molecular design that is simpler to implement than that of designer phthalocyanines such as **La Jolla Blue**. The ability to solubilize large hydrophobic organic compounds by straightforward attachment to a heterotelechelic, amphiphilic polymer should find applications across the life sciences.

Experimental Section

General Methods. All chemicals obtained commercially were used as received unless noted otherwise. HPLC-grade solvents (toluene, DMF, water) were used in absorption, fluorescence, and DLS spectroscopy, as well as in analytical SEC. In all other cases, solvents were reagent-grade and used as received unless noted otherwise. THF was freshly distilled from sodium/benzophenone ketyl and used immediately. Electrospray ionization mass spectrometry (ESI-MS) data are reported for the molecular ion or cationized molecular ion. The monomers **PEGA** and **LA** were used as received. **AMPS** was received as an aqueous solution, which was treated with NaOH until the pH was slightly > 7, and then dried under high vacuum to afford a white solid.

Non-commercial compounds. Perylene **PMI-Br**,[43] chlorin **1**,[39] chlorin **Chl-Br**,[40] and phthalocyanine **ZnPc(*t*-Bu)$_3$-NH$_2$**[44] were prepared as described in the literature. Fluorescence benchmarks include **Chl-TM**[45,48] and **ZnPc(*t*-Bu)$_4$**.[49]

Absorption Spectroscopy.[30] Absorption spectra were measured with a diode-array instrument using dilute (μmolar) solutions of the compound in 1-cm pathlength cuvettes versus a solvent blank at room temperature. Fluorophore–polymer samples were dissolved in HPLC-grade water containing 1.0 M NaCl (filtered with a 220-nm membrane) and the resulting solutions were passed through the 220-nm membrane prior to analysis. The fluorophore benchmarks were dissolved in HPLC-grade toluene for analysis. All measurements that are stated to take place in aqueous solution refer to aqueous NaCl (1.0 M) solution.

Fluorescence Spectroscopy.[30] Fluorescence spectra were measured 2–4 nm excitation and detection bandwidths and corrected for instrument spectral response using dilute (μmolar) solutions in 1-cm pathlength cuvettes. Fluorescence quantum yields were obtained by ratio with known standards. No correction was made for the refractive index of different media. All measurements in aqueous solution refer to aqueous NaCl (1.0 M) solution unless noted otherwise.

Dynamic Light Scattering (DLS) Spectroscopy.[30] DLS analysis was performed in 1-cm pathlength cuvettes with a Zetasizer Nano ZS instrument. Sample preparation was as follows: a polymer or fluorophore–polymer sample was dissolved in HPLC-grade water containing 1.0 M NaCl (filtered with a 220-nm membrane) and passed through a 220-nm membrane to make defined concentrations (1–10 mg/mL) for analysis. Illumination was performed at 632.8 nm. All measurements that are stated to take place in aqueous solution refer to aqueous NaCl (1.0 M) solution unless noted otherwise.

Nuclear Magnetic Resonance (NMR) Spectroscopy. ^{1}H NMR spectra were measured at 700 MHz at room temperature unless otherwise noted.

General Methods for Sample Dialysis.[30] A membrane tubing with appropriate length (Spectra/Por® Regenerated Cellulose Membranes, molecular weight cut off at 3.5 kDa) was soaked in deionized (DI) water for 30 min to remove any cellulose and sodium azide from the membrane. Then, the membrane was rinsed with DI water. A magnetic closure was clamped onto the bottom of the membrane tubing. A crude polymer sample in DI water or DMF (reagent grade) was transferred into the membrane tubing. The second closure at the top of the tubing was then clamped, leaving sufficient headspace to cause the tube to float in the dialysis liquid (DI water or DMF). The closed tubing containing the sample was placed into a dialysis reservoir (containing ~100-times the volume of the sample) equipped with a magnetic stir-bar. The tubing was then stirred in the dialysis solution at room temperature. The reservoir volume was typically replaced with fresh DI water (for polymer synthesis; or DMF for fluorophore–polymer conjugations) at intervals of ~2 h during the course of the day, allowed to proceed overnight, and then changed again to give a total of four changes of the dialysis reservoir solvent. The dialyzed sample solution was transferred from the membrane tubing to a glass vial and dried under high vacuum to give the desired polymer product.

Coumarin-hydrazide. Following a reported procedure,[38] a solution of **Coumarin 314** (50. mg, 0.16 mmol) in ethanol (9.0 mL) was treated with hydrazine hydrate (0.50 mL, 8.0 mmol) at 0 °C. The mixture was stirred at 0 °C for 2 h, whereupon the solution was cooled to –20 °C. The precipitate was filtered and washed with cold ethanol. The resulting precipitate was dried to afford an orange solid (30 mg, 63%): ^{1}H NMR ($CDCl_3$, 700 MHz) δ 9.76 (s, 1H), 8.55 (s, 1H), 6.99 (s, 1H), 4.14 (br, 2H), 3.49–3.32 (m, 4H), 2.87 (t, J = 6.5 Hz, 2H), 2.77 (t, J = 6.4 Hz, 2H), 2.02–1.92 (m, 4H); ^{13}C NMR ($CDCl_3$, 175 MHz) δ 164.3, 162.4, 152.6, 148.3, 147.9, 127.0, 119.7, 108.9, 107.6, 150.7, 50.2, 49.8, 27.5, 21.1, 20.1, 20.0; ESI-MS: obsd 300.13427 [$(M + H)^+$], calcd 300.13361 ($M = C_{16}H_{17}N_3O_3$).

Coumarin-hydrazone. A solution of **Coumarin-hydrazide** (5.5 mg, 0.018 mmol) and *p*-tolualdehyde (2.4 mg, 0.020 mmol) in CH_2Cl_2 (1.1 mL) was stirred at room temperature for 16 h. The mixture was dried and purified by column chromatography [silica, CH_2Cl_2 to CH_2Cl_2/MeOH (95:5, v/v)] to give an orange solid (6.8 mg, 94%): ^{1}H NMR ($CDCl_3$, 700 MHz) δ 11.91 (s, 1H), 8.74 (s, 1H), 8.18 (s, 1H), 7.73 (s, J = 7.9 Hz, 2H), 7.23 (d, J = 7.8 Hz, 2H), 7.06 (s, 1H), 3.41–3.32 (m, 4H), 2.93 (t, J = 6.4 Hz, 2H), 2.80 (t, J = 6.3 Hz, 2H), 2.40 (s, 3H), 2.06–1.96 (m, 4H);

^{13}C NMR ($CDCl_3$, 175 MHz) δ 163.1, 160.3, 152.8, 149.0, 148.6, 148.4, 140.6, 131.2, 129.3, 127.8, 127.3, 120.0, 108.5, 107.6, 105.7, 50.3, 49.9, 27.5, 21.6, 21.1, 20.13, 20.09; ESI-MS: obsd 402.18122 [$(M + H)^+$], calcd 402.18088 ($M = C_{24}H_{23}N_3O_3$).

9-(4-Aminophenyl)-*N*-(2,6-diisopropylphenyl)-1,6-bis(4-*tert*-butylphenoxy)-perylene-3,4-dicarboximide (PMI-NH_2). According to a reported procedure,[42] **PMI-Br** (40. mg, 47 μmol), 4-aminobenzeneboronic acid pinacol ester (**3**, 21 mg, 94 μmol), Pd(dppf)Cl_2 (1.8 mg, 2.4 μmol), and KOAc (12 mg, 0.12 mmol) were placed in a Schlenk flask. The flask was deaerated by three vacuum-purge cycles with argon. Then toluene (1.4 mL, bubbled with argon) was added to the flask under a stream of argon. The resulting solution was deaerated by three freeze-pump-thaw cycles. The mixture was stirred at 90 °C for 16 h. The mixture was allowed to cool to room temperature and washed with water. The resulting mixture was extracted with CH_2Cl_2, and the organic extract was dried (Na_2SO_4), concentrated, and purified by column chromatography [silica, hexanes/CH_2Cl_2 (1:1 v/v to 1:3 v/v)] to give a dark purple solid (17 mg, 43%): ^{1}H NMR ($CDCl_3$, 700 MHz) δ 9.35 (d, J = 3.0 Hz, 2H), 8.33 (s, 2H), 8.10 (d, J = 8.6 Hz, 1H), 7.52 (t, J = 8.3 Hz, 2H), 7.43 (t, J = 7.9 Hz, 1H), 7.41–7.36 (m, 4H), 7.34–7.30 (m, 2H), 7.29 (d, J = 7.9 Hz, 2H), 7.07 (t, J = 8.3 Hz, 4H), 6.83–6.72 (m, 2H), 3.82 (s, 2H), 2.72 (hept, J = 6.7 Hz, 2H), 1.33 (s, 18 H), 1.14 (d, J = 6.9 Hz, 12H); ^{13}C NMR ($CDCl_3$, 175 MHz) δ 163.3, 153.5, 153.2, 153.1, 147.0, 146.2, 145.7, 142.8, 131.92, 131.86, 131.2, 130.8, 130.2, 130.0, 129.4, 129.1, 128.9, 128.7, 127.9, 127.80, 127.76, 127.7, 127.1, 126.39, 126.36, 124.7, 123.9, 123.4, 121.3, 121.1, 118.3, 115.0, 34.4, 31.5, 29.7, 29.1, 24.0; ESI-MS obsd 869.42913, [$(M + H)^+$], calcd 869.43128 ($M = C_{60}H_{56}N_2O_4$).

***N*-(2,6-Diisopropylphenyl)-1,6-bis(4-*tert*-butylphenoxy)-9-(4-(3-(2,5-dioxo-2,5-dihydro-1*H*-pyrrole-1-carboxamido)propylcarbamoyl)phenyl)-perylene-3,4-dicarboximide (PMI-mal).** According to a reported procedure,[41] **Mal-acid** (1.4 mg, 6.0 μmol) in CH_2Cl_2 (215 μL) was treated with EDC (11 mg, 0.058 mmol). The resulting mixture was stirred at room temperature for 1 h, whereupon **PMI-NH_2** (5.0 mg, 5.8 μmol) was added to the solution. The reaction mixture was stirred at room temperature for 16 h. The mixture was diluted with CH_2Cl_2 and washed with water. The organic layer was dried (Na_2SO_4), concentrated, and purified by column chromatography [silica, CH_2Cl_2 to CH_2Cl_2/methanol (99:1)] to give a pink solid (4.7 mg, 76%): ^{1}H NMR ($CDCl_3$, 700 MHz, one of the NH protons was not observed) δ 9.38 (t, J = 8.1 Hz, 2H), 8.36 (s, 2H), 8.10–8.01 (m, 2H), 7.76 (d, J = 8.0 Hz, 2H), 7.56 (dd, J = 8.3, 6.7 Hz, 2H), 7.52 (d, J = 8.1 Hz, 2H), 7.46 (t, J = 7.9 Hz, 1H), 7.44–7.40 (m, 4H), 7.32 (d, J = 7.9 Hz, 2H), 7.13–7.08 (m, 4H), 6.78 (s, 2H), 3.72 (t, J = 6.2 Hz, 2H), 2.75 (hept, J = 6.9 Hz, 2H), 2.41 (t, J = 6.8

Hz, 2H), 2.10 (p, J = 6.4 Hz, 2H), 1.36 (s, 18 H), 1.17 (d, J = 6.9 Hz, 12H); ^{13}C NMR ($CDCl_3$, 175 MHz) δ 171.3, 170.3, 163.2, 153.43, 153.39, 153.36, 147.1, 147.0, 145.7, 137.6, 136.0, 134.3, 131.9, 131.8, 130.8, 130.7, 129.9, 129.4, 128.9, 128.7, 128.5, 127.9, 127.8, 127.7, 127.4, 127.13, 127.11, 127.0, 126.7, 124.6, 124.5, 123.9, 123.3, 121.5, 121.3, 119.7, 118.3, 37.0, 34.9, 34.4, 31.5, 29.7, 29.1, 25.3, 24.0, 22.7, 14.1; ESI-MS obsd 1033.46605 $(M)^+$, calcd 1033.46582 (M = $C_{68}H_{63}N_3O_7$).

10-Mesityl-5-[(4-methoxycarbonyl)phenyl]-18,18-dimethylchlorin (2). Toluene and methanol were deaerated by bubbling with argon for 1 h. A conical vial with a rubber septum was charged with iodochlorin **1** (20 mg, 0.030 mmol, 1.0 equiv) and $Pd(PPh_3)_4$ (3.5 mg, 3.0 μmol, 0.10 equiv), and then evacuated under high vacuum. The vial was then refilled with argon. This evacuation-purge process was repeated three times. The deaerated toluene (0.50 mL) and methanol (0.50 mL) were added to the vial under argon, as well as triethylamine (21 μL, 0.15 mmol, 5.0 equiv). The solution was deaerated again with three freeze-pump-thaw cycles. The vial was evacuated under high vacuum at 77 K, and then refilled with carbon monoxide. A balloon full of CO was also connected to the vial to provide extra pressure. The solution was stirred at 65 °C for 23 h, concentrated and chromatographed (silica, hexanes/CH_2Cl_2 = 1:1) to afford a green solid (18 mg, 100%): TLC (silica, hexanes/CH_2Cl_2 = 1:1) R_f = 0.28; ^{1}H NMR ($CDCl_3$, 300 MHz) δ 8.92 (s, 1H), 8.87 (s, 1H), 8.82 (d, J = 4.8 Hz, 1H), 8.73 (d, J = 4.7 Hz, 1H), 8.69 (d, J = 4.7 Hz, 1H), 8.61 (d, J = 4.7 Hz, 1H), 8.38 (d, J = 8.1 Hz, 2H), 8.37 (s, 1H), 8.36 (s, 1H), 8.22 (d, J = 8.3 Hz, 2H), 7.22 (s, 2H), 4.57 (s, 2H), 4.08 (s, 3H), 2.58 (s, 3H), 2.03 (s, 6H), 1.84 (s, 6H), –1.87 (br, s, 2H); ^{13}C NMR ($CDCl_3$, 100 MHz) δ 175.2, 167.6, 163.6, 152.4, 151.5, 147.2, 140.9, 140.4, 139.2, 138.3, 137.7, 134.7, 134.4, 134.1, 132.1, 131.1, 129.5, 128.1, 128.0, 127.8, 123.7, 123.6, 120.59, 120.57, 96.81, 94.99, 52.49, 51.86, 46.63, 31.31, 21.57, 21.45; MALDI-MS obsd 593.1 $[(M + H)^+]$, calcd 592.3 (M = $C_{39}H_{36}N_4O_2$); λ_{abs} (CH_2Cl_2) 415, 509, 533, 590, 641 nm.

5-[4-(*N*-Aminocarbamoyl)phenyl]-10-mesityl-18,18-dimethylchlorin (Chl-hydrazide). A solution of chlorin **2** (44 mg, 75 μmol, 1.0 equiv) in THF (1.0 mL) was treated with methanol (1.0 mL) and hydrazine hydrate (0.21 mL, 3.8 mmol, 50 equiv) at 50 °C for 24 h. [Note: Reduction of the chlorin-hydrazine to the corresponding bacteriochlorin-hydrazine ensued at concentrations > 50 mM. The bacteriochlorin could be dehydrogenated to give the desired chlorin by treatment with DDQ (1.0 equiv) in CH_2Cl_2 at room temperature for 30 min.] The solution was then diluted with ethyl acetate, washed with water, dried (Na_2SO_4), concentrated and chromatographed (silica, hexanes/ethyl acetate = 1:2 to CH_2Cl_2/CH_3OH = 9:1) to afford a green solid (37 mg, 84%): ^{1}H

NMR (700 MHz, THF-d_8) δ 9.04 (s, 1H), 9.02 (s, 1H), 8.94 (d, J = 4.6 Hz, 1H), 8.85 (d, J = 4.6 Hz, 1H), 8.71 (d, J = 4.6 Hz, 1H), 8.56 (d, J = 4.6 Hz, 1H), 8.39 (d, J = 8.0 Hz, 2H), 8.35 (d, J = 4.3 Hz, 1H), 8.27 (d, J = 4.3 Hz, 1H), 8.21 (d, J = 8.0 Hz, 2H), 7.19 (t, J = 7.6 Hz, 1H), 7.13 (d, J = 7.5 Hz, 1H), 4.73 (s, 2H), 4.65 (s, 2H), 2.58 (s, 3H), 2.08 (s, 6H), 1.83 (s, 6H), –1.75 (s, 1H), –1.83 (s, 1H); MALDI-MS obsd 593.1 [(M + H)$^+$], calcd 592.3 (M = $C_{38}H_{36}N_6O$). A ^{13}C NMR spectrum could not be obtained due to low solubility.

15-(4-Aminophenyl)-10-mesityl-18,18-dimethyl-5-(4-methylphenyl)chlorin (Chl-NH$_2$). Following a reported procedure,[39] samples of 15-bromo-10-mesityl-18,18-dimethyl-5-(4-methylphenyl)chlorin (**Chl-Br**, 38 mg, 60 μmol), 4-aminobenzeneboronic acid pinacol ester (**3**, 26 mg, 0.12 mmol), $Pd(PPh_3)_4$ (17 mg, 15 μmol), and Cs_2CO_3 (106 mg, 0.30 mmol) were placed in a Schlenk flask. The mixture was deaerated by three vacuum-purge (argon) cycles. Then deaerated DMF/toluene (1.8 mL, 3:1, v/v) was added to the flask under a stream of argon. The resulting solution was deaerated by three freeze-pump-thaw cycles and then stirred at 90 °C for 16 h. The mixture was allowed to cool to room temperature and diluted with CH_2Cl_2. The organic solution was washed with brine, dried over Na_2SO_4, concentrated and chromatographed (silica, CH_2Cl_2) to afford a brown solid (18 mg, 47%): ^{1}H NMR ($CDCl_3$, 700 MHz) δ 8.89 (s, 1H), 8.86–8.82 (m, 2H), 8.53–8.51 (m, 2H), 8.38–8.37 (m, 1H), 8.35–8.34 (m, 1H), 8.09 (d, J = 7.0 Hz, 2H), 7.71 (d, J = 7.0 Hz, 2H), 7.55 (d, J = 6.3 Hz, 2H), 7.26–7.25 (m, 2H), 6.99 (s, 2H), 4.28 (s, 2H), 3.88 (s, 2H), 2.70 (s, 3H), 2.63 (s, 3H), 2.02 (s, 6H), 1.91 (s, 6H), –1.42 (s, 1H), –1.70 (s, 1H); ^{13}C NMR ($CDCl_3$, 175 MHz) δ 174.4, 163.5, 152.7, 151.8, 145.7, 141.4, 140.4, 139.2, 138.9, 137.3, 137.2, 135.5, 134.13, 134.08, 133.3, 132.9, 132.2, 131.0, 128.2, 127.63, 127.58, 127.0, 123.6, 123.5, 121.6, 120.7, 114.6, 111.9, 94.9, 52.1, 45.9, 31.4, 21.4; ESI-MS obsd 640.34244 [(M + H)$^+$], calcd 640.34347 (M = $C_{44}H_{41}N_5$).

10-Mesityl-18,18-dimethyl-15-[4-(3-(2,5-dioxo-2,5-dihydro-1*H*-pyrrole-1-carboxamido)propylcarbamoyl)phenyl]-5-(4-methylphenyl)chlorin (Chl-mal). Following a reported procedure,[41] a mixture of **Mal-acid** (3.1 mg, 17 μmol) and EDC (32 mg, 0.17 mmol) in DMF (500 μL) was stirred at room temperature for 1 h, whereupon chlorin **Chl-NH$_2$** (9.0 mg, 14 μmol was added to the solution. The mixture was stirred at room temperature for 16 h. The resulting mixture was a diluted with CH_2Cl_2. The organic solution was washed with water and brine, dried over Na_2SO_4, concentrated and chromatographed (silica, CH_2Cl_2) to afford a violet solid (5.0 mg, 44%): ^{1}H NMR ($CDCl_3$, 700 MHz, the amide N-H proton was not observed) δ 8.83 (s, 1H), 8.81 (d, J = 4.6 Hz, 1H), 8.77 (d, J = 4.6 Hz, 1H), 8.45 (d, J = 4.4 Hz, 2H), 8.30 (d, J =

4.3 Hz, 1H), 8.22 (d, J = 4.8 Hz, 1H), 8.19 (s, 1H), 8.03 (s, 1H), 2.03 (s, 1H), 7.91 (d, J = 8.0 Hz, 2H), 7.87 (d, J = 8.0 Hz, 2H), 7.51 (d, J = 7.5 Hz, 2H), 7.21 (s, 2H), 6.79 (s, 2H), 4.19 (s, 2H), 3.78 (t, J = 6.2 Hz, 2H), 2.67 (s, 4H), 2.58 (s, 3H), 2.48 (t, J = 6.9 Hz, 2H), 1.96 (s, 6H), 1.84 (s, 6H), –1.48 (s, 1H), –1.73 (s, 1H); ^{13}C NMR ($CDCl_3$, 175 MHz) δ 174.5, 171.3, 170.4, 162.5, 152.8, 151.7, 140.8, 140.5, 139.1, 138.8, 137.3, 137.1, 135.6, 134.3, 133.99, 133.95, 133.0, 132.1, 131.0, 128.3, 127.6, 127.5, 127.0, 123.5, 121.6, 121.0, 119.2, 111.1, 94.8, 52.0, 46.0, 37.1, 34.9, 31.3, 29.7, 25.4, 21.5, 21.4, 21.3, 14.1; ESI-MS obsd 805.38534 [$(M + H)^+$], calcd 805.38607 (M = $C_{52}H_{48}N_6O_3$).

ZnPc(*t*-Bu)$_3$-mal. A solution of **ZnPc(*t*-Bu)$_3$-NH$_2$** (33.0 mg, 42.6 μmol) and **Mal-acid** (11.7 mg, 63.9 μmol) in anhydrous 1,4-dioxane (0.8 mL) was treated with DCC (43.9 mg, 0.213 mmol) under argon. The reaction mixture was stirred at room temperature for 15 h. The starting phthalocyanine (**ZnPc(*t*-Bu)$_3$-NH$_2$**) was unstable and reverted to its precursor, the corresponding nitro-phthalocyanine **ZnPc(*t*-Bu)$_3$-NO$_2$**, during the reaction. TLC analysis [silica, hexanes:1,4-dioxane (2:1)] of the crude mixture showed the title compound at R_f = 0.2 and the nitro-phthalocyanine **ZnPc(*t*-Bu)$_3$-NO$_2$** near the solvent front. No starting phthalocyanine **ZnPc(*t*-Bu)$_3$-NH$_2$**, which migrates at an R_f intermediate between that of **ZnPc(*t*-Bu)$_3$-NO$_2$** and the title compound, was observed. The **Mal-acid** remains at the origin of the TLC plate. The crude mixture was concentrated and purified by preparative column chromatography under the same conditions [silica, hexanes:1,4-dioxane (2:1)] as those for the TLC analysis to afford a green-blue solid (16.0 mg, 40%). Attempted NMR characterization in pyridine-d_5 or THF-d_8 was not successful. ESI-MS obsd 925.3237 [$(M + H)^+$], calcd 925.3275 (M = $C_{52}H_{48}N_{10}O_3Zn$); λ_{abs} = 680 nm (toluene).

Synthesis of the new batch of F-Ph. Following a reported procedure,[30] a solution of **AMPS** (2.52 g, 11.0 mmol), **PEGA** (1.06 g, 2.19 mmol), **LA** (532 mg, 2.20 mmol), 4-cyano-4-(phenylcarbonothioylthio)pentanoic acid (16.8 mg, 0.060 mmol) and mesitylene (220 mg, 1.83 mmol) in DMF (18.0 mL) was deaerated by three freeze-pump-thaw cycles in a Schlenk flask. Then, AIBN (3.2 mg, 0.020 mmol) was added to the flask. The mixture was stirred at 80 °C for 24 h. After that, ^{1}H NMR analysis showed 85%, 83% and 81% conversion for **AMPS**, **PEGA** and **LA**, respectively; these values are considered to be within experimental error of each other. The mixture was allowed to cool to room temperature and then poured into 500 mL of diethyl ether. The resulting precipitate was washed twice with diethyl ether and dried under high vacuum. The crude polymer was dissolved in DI water (~300 mg of polymer in 10 mL of DI water) and placed

in a dialysis membrane tubing equipped with two closures. The reservoir volume was replaced with fresh DI water 4 times over the course of ~24 h. The resulting dialyzed polymer solution was freeze-dried under high vacuum to yield a light pink solid (~1.90 g): ^{1}H NMR (CD_3OD, 700 MHz) δ 8.09–7.94 (aromatic), 7.60–7.48 (aromatic), 4.40–4.00 (-$CO_2C\underline{H}_2$-), 3.86–3.62 (-$OC\underline{H}_2C\underline{H}_2O$-, -$C\underline{H}_2SO_3Na$), 3.61–3.54 (-$OC\underline{H}_2C\underline{H}_2O$-), 3.42–3.36 (-$OCH_2CH_2OC\underline{H}_3$), 2.50–2.05 (-$CO_2C\underline{H}(C\underline{H}_2)_2$-), 1.90–1.73 (-$CO_2CH_2C\underline{H}_2CH_2$-), 1.74–1.43 (-$(C\underline{H}_3)_2CH_2SO_3Na$), 1.42–1.25 (-$CO_2CH_2CH_2(C\underline{H}_2)_9CH_3$), 0.94–0.88 (-$CO_2CH_2(CH_2)_{10}C\underline{H}_3$); $Đ$ (M_w/M_n) = 1.55.

Fluorophore–Pods. Pod-Chl-hydrazone and **Pod-PMI** were prepared previously from the first batch of **F-Ph** where m, n, and p ~ 20, 20, and 100, respectively, with M_n = 40 kDa.[30] **Pod-Chl** was prepared here using the first batch[30] of **F-Ph**. **Pod-ZnPc(*t*-Bu)$_3$** was prepared here using the second batch of **F-Ph** where m, n, and p ~ 18, 18, and 90, respectively, with M_n = 36 kDa.

General Method for Reaction of Fluorophore–Maleimides with F-Ph, Illustrated for Pod-ZnPc(*t*-Bu)$_3$. Following a reported procedure,[30] a solution of **F-Ph** (new batch, 19 mg, 0.49 μmol) and **ZnPc(*t*-Bu)$_3$-mal** (1.0 mg, 1.1 μmol) in DMF (300 μL) was treated with ethanolamine (1 drop). The resulting mixture was stirred at 30 °C for 10 h. Then the mixture was transferred to a dialysis membrane tubing equipped with two closures. The solution was dialyzed in DMF, and the dialysis reservoir volume was replaced with fresh DMF four times over the course of ~24 h. The resulting dialyzed solution was dried under high vacuum at 50 °C, and the resulting solid was dissolved in DI water. The aqueous solution was freeze-dried to give a green solid (18 mg).

Pod-Chl. Following the method described for **Pod-ZnPc(*t*-Bu)$_3$**, samples of **F-Ph** (previous batch,[30] 124 mg), **Chl-mal** (3.0 mg, 3.7 μmol), and ethanolamine (0.80 μL, 15 μmol) were reacted in DMF (400 μL) to give a red solid (120 mg).

Conflict of Interest Statement: J.S.L. is cofounder of NIRvana Sciences, which develops fluorophores for use in clinical diagnostics. Patent applications concerning some of the present material have been licensed to NIRvana Sciences.

Acknowledgements

Exploratory work (2014–2018) leading to the present paper was supported by the Photosynthetic Antenna Research Center (PARC), an Energy Frontier Research Center funded by the U.S. Department of Energy, Office of Science, Office of Basic Energy Sciences, under Award No. DE-

SC0001035. Studies of **F-Ph** and derivatives (2018–2020) were supported by a grant (2R44AI112302-04A1) to NIRvana Sciences from the NIGMS. Mass spectrometry and NMR spectroscopy were carried out in the Molecular Education, Technology, and Research Innovation Center (METRIC) at NC State University.

Electronic Supplementary Information.

Characterization data for **F-Ph**; absorption and fluorescence data for **PMI-mal** in various solvents; and ^{1}H and ^{13}C NMR spectral data (where available) for new compounds.

ORCID numbers

Rui Liu: 0000-0003-2927-3080

Sijia Liu: 0000-0003-3898-7966

Gongfang Hu: 0000-0002-0387-9079

Jonathan S. Lindsey: 0000-0002-4872-2040

Footnote †

The appellation "single-cargo–single-polymer" is accurate albeit quite general. The specific constructs here are fluorophore–polymers, with one fluorophore per polymer, and are also termed fluorophore–SCNPs to denote the folding properties of the polymer. We previously have used the term "Pod" to reflect the notion of an SCNP that encapsulates the single cargo entity.[30] Accordingly, the term fluorophore–Pod and fluorophore–SCNP are used equivalently here for consistency.

References

1 A. X. P. D'mello, T. V. Sylvester, V. Ramya, F. P. Britto, P. K. Shetty and S. Jasphin, *Int. J. Adv. Health Sci.,* 2016, **2(10)**, 12–17.

2 A. Waggoner, R. DeBiasio, P. Conrad, G. R. Bright, L. Ernst, K. Ryan, M. Nederlof and D. Taylor, *Methods Cell Biol*., 1989, **30**, 449−478.

3 M. Taniguchi, G. Hu, R. Liu, H. Du and J. S. Lindsey, *Proc. S.P.I.E. BiOS*, 2018, **Vol. 10508**, Reporters, Markers, Dyes, Nanoparticles, and Molecular Probes for Biomedical Applications X, 1050806.

4 R. W. Wagner and J. S. Lindsey, *Pure Appl. Chem.*, **1996**, *68*, 1373–1380. Corrigendum: R. W. Wagner and J. S. Lindsey, *Pure Appl. Chem.*, 1998, **70 (8)**, p. i.

5 P. L. Southwick, L. A. Ernst, E. W. Tauriello, S. R. Parker, R. B. Mujumdar, S. R. Mujumdar, H. A. Clever and A. S. Waggoner, *Cytometry*, 1990, **11**, 418–430.

6 R. Devlin, R. M. Studholme, W. B. Dandliker, E. Fahy, K. Blumeyer and S. S. Ghosh, *Clin. Chem.*, 1993, **39**, 1939–1943.

7 W. B. Dandliker and M.-L. Hsu, US Patent 5,919,922.

8 W. B. Dandliker, M.-L. Hsu and W. P. Murphy, Jr., US Patent 7,371,524.

9 M. Luciano and C. Brückner, *Molecules*, 2017, **22**, 980.

10 A. Z. Muresan and J. S. Lindsey, *Tetrahedron*, 2008, **64**, 11440–11448.

11 J. S. Lindsey, *Chem. Rev.*, 2015, **115**, 6534–6620.

12 N. Matsumoto, M. Taniguchi and J. S. Lindsey, *J. Porphyrins Phthalocyanines*, 2020, **24**, 362–378.

13 J. Jiang, E. Yang, K. R. Reddy, D. M. Niedzwiedzki, C. Kirmaier, D. F. Bocian, D. Holten and J. S. Lindsey, *New J. Chem.*, 2015, **39**, 5694–5714.

14 A. M. Breul, M. D. Hager and U. S. Schubert, *Chem. Soc. Rev*., 2013, **42**, 5366–5407.

15 O. S. Wolfbeis, *Chem. Soc. Rev.*, 2015, **44**, 4743–4768.

16 M. P. Robin and R. K. O'Reilly, *Polym. Int.*, 2015, **64**, 174–182.

17 A. M. Hanlon, C. K. Lyon and E. B. Berda, *Macromolecules*, 2016, **49**, 2−14.

18 A. Reisch and A. S. Klymchenko, *Small*, 2016, **12**, 1968–1992.

19 O. Altintas and C. Barner-Kowollik, *Macromol. Rapid Commun.*, 2016, **37**, 29–46.

20 J. De-La-Cuesta, E. González and J. A. Pomposo, *Molecules*, 2017, **22**, 1819.

21 E. Blasco, B. T. Tuten, H. Frisch, A. Lederer and C. Barner-Kowollik, *Polym. Chem.*, 2017, **8**, 5845–5851.

22 J. Rubio-Cervilla, E. González and J. A. Pomposo, *Nanomaterials*, 2017, **7**, 341.

23 J. Engelke, J. Brandt, C. Barner-Kowollik and A. Lederer, *Polym. Chem.*, 2019, **10**, 3410–3425.

24 K. Li and B. Liu, *Chem. Soc. Rev*., 2014, **43**, 6507–6597.

25 J. Yu, Y. Rong, C.-T. Kuo, X.-H. Zhou and D. T. Chiu, *Anal. Chem.*, 2017, **89**, 42−56.

26 Y. Morishima, S. Nomura, T. Ikeda, M. Seki and M. Kamachi, *Macromolecules*, 1995, **28**, 2874–2881.

27 T. Terashima, T. Sugita, K. Fukae and M. Sawamoto, *Macromolecules*, 2014, **47**, 589−600.

28 M. Matsumoto, T. Terashima, K. Matsumoto, M. Takenaka and M. Sawamoto, *J. Am. Chem. Soc.*, 2017, **139**, 7164−7167.

29 S. Imai, Y. Hirai, C. Nagao, M. Sawamoto and T. Terashima, *Macromolecules*, 2018, **51**, 398−409.

30 R. Liu and J. S. Lindsey, *ACS Macro Lett.*, 2019, **8**, 79–83. Erratum: *ACS Macro Lett.*, 2019, **8**, 154.

31 F. M. Winnik, *Chem. Rev.*, 1993, **93**, 587–614.

32 J. Chiefari, Y. K. Chong, F. Erocle, J. Krstina, J. Jeffery, T. P. T. Le, R. T. A. Mayadunne, G. F. Meijs, C. L. Moad, G. Moad, E. Rizzardo and S. H. Thang, *Macromolecules*, 1998, **31**, 5559–5562.

33 M. Semsarilar and S. Perrier, *Nat. Chem.*, 2010, **2**, 811−820.

34 D. J. Keddie, *Chem. Soc. Rev.*, 2014, **43**, 496−505.

35 S. Perrier, *Macromolecules*, 2017, **50**, 7433–7447.

36 R. Liu, P. Vairaprakash and J. S. Lindsey, *New J. Chem.*, 2019, **43**, 9711–9724.

37 M. A. Harris, T. Sahin, J. Jiang, P. Vairaprakash, P. S. Parkes-Loach, D. M. Niedzwiedzki, C. Kirmaier, P. A. Loach, D. F. Bocian, D. Holten and J. S. Lindsey, *Photochem. Photobiol.*, 2014, **90**, 1264–1276.

38 B. Epe, K. G. Steinhäuser and P. Woolley, *Proc. Natl. Acad. Sci. USA*, 1983, **80**, 2579–2583.

39 R. Liu, M. Liu, D. Hood, C.-Y. Chen, C. J. MacNevin, D. Holten and J. S. Lindsey, *Molecules*, 2018, **23**, 130.

40 M. Taniguchi, M. N. Kim, D. Ra and J. S. Lindsey, *J. Org. Chem.*, 2005, **70**, 275–285.

41 K. R. Reddy, J. Jiang, M. Krayer, M. A. Harris, J. W. Springer, E. Yang, J. Jiao, D. M. Niedzwiedzki, D. Pandithavidana, P. S. Parkes-Loach, C. Kirmaier, P. A. Loach, D. F. Bocian, D. Holten and J. S. Lindsey, *Chem. Sci.*, 2013, **4**, 2036–2053.

42 G. Hu, R. Liu, E. J. Alexy, A. K. Mandal, D. F. Bocian, D. Holten and J. S. Lindsey, *New J. Chem.*, 2016, **40**, 8032–8052.

43 P. Schlichting, B. Duchscherer, G. Seisenberger, T. Basché, C. Bräuchle and K. Müllen, *Chem. Eur. J.*, 1999, **5**, 2388–2395.

44 J. M. Sutton and R. W. Boyle, *Chem. Commun.*, 2001, 2014–2015.

45 J.-P. Strachan, D. F. O'Shea, T. Balasubramanian and J. S. Lindsey, *J. Org. Chem.*, 2000, **65**, 3160–3172.

46 R. L. Hinman, *J. Org. Chem.*, 1960, **25**, 1775–1778.

47 S. I. Yang, J. Li, H. S. Cho, D. Kim, D. F. Bocian, D. Holten and J. S. Lindsey, *J. Mater. Chem.*, 2000, **10**, 283–296.

48 K. Aravindu, H.-J. Kim, M. Taniguchi, P. L. Dilbeck, J. R. Diers, D. F. Bocian, D. Holten and J. S. Lindsey, *Photochem. Photobiol. Sci.*, 2013, **12**, 2089–2109.

49 M. E. Rodriguez, V. E. Diz, J. Awruch and L. E. Dicelio, *Photochem. Photobiol.*, 2010, **86**, 513–519.

50 H. Kamogawa, *J. Polym. Sci. Polym. Chem.*, 1974, **12**, 2317–2325.

51 M. Kamachi, H. Akimoto and S.-i. Nozakura, *J. Polym. Sci. Polym. Lett.*, 1983, **21**, 693–698.

52 K. Shigehara, K.-I. Shinohara, Y. Sato and E. Tsuchida, *Macromolecules*, 1981, **14**, 1153–1161.

53 W. Lautsch, W. Broser, W. Rothkegel, W. Biedermann, U. Doering and H. Zoschke, *J. Polym. Sci.*, 1952, **8**, 191–213.

54 W. Lautsch, W. Broser, W. Biedermann, H. Gnichtel, *J. Polym. Sci.*, 1955, **17**, 479–510.

55 R. A. Cellarius and D. Mauzerall, *Biochim. Biophys. Acta*, 1966, **112**, 235–255.

56 M. A. Tasdelen, M. U. Kahveci and Y. Yagci, *Prog. Polym. Sci.*, 2011, **36**, 455–567.

57 P. J. Roth, C. Boyer, A. B. Lowe and T. P. Davis, *Macromol. Rapid Commun*., 2011, **32**, 1123–1143.

58 M. Beija, M.-T. Charreyre and J. M. G. Martinho, *Prog. Polym. Sci.*, 2011, **36**, 568–602.

59 C. W. Scales, A. J. Convertine and C. L. McCormick, *Biomacromolecules*, 2006, **7**, 1389–1392.

60 A. W. York, C. W. Scales, F. Huang and C. L. McCormick. *Biomacromolecules*, 2007, **8**, 2337–2341.

61 P. J. Roth, K.-S. Kim, S. H. Bae, B.-H. Sohn, P. Theato and R. Zentel, *Macromol. Rapid Commun*., 2009, **30**, 1274–1278.

62 H. Li, B. Yu, H. Matsushima, C. E. Hoyle and A. B. Lowe, *Macromolecules*, 2009, **42**, 6537–6542.

63 J. Liu, W. Yang, L. Tao, D. Li, C. Boyer and T. P. Davis, *J. Polym. Sci.: Part A: Polym. Chem.*, 2010, **48**, 425–433.

64 J. Madsen, N. J. Warren and S. P. Armes, *Biomacromolecules*, 2011, **12**, 2225–2234.

65 F. Biedermann, E. A. Appel, J. del Barrio, T. Gruendling, C. Barner-Kowollik and O. A. Scherman, *Macromolecules*, 2011, **44**, 4828–4835.

66 M. Liras, O. García, I. Quijada-Garrido and R. París, *Macromolecules*, 2011, **44**, 1335–1339.

67 M. Beija, C. A. M. Afonso, J. P. S. Farinha, M.-T. Charreyre and J. M. G. Martinho, *Polymer*, 2011, **52**, 5933–5946.

68 J. Liu, J. Tanga and J. J. Gooding, *J. Mater. Chem*., 2012, **22**, 12435–12452.

69 M. Wolff, D. Braun and M. A. Nash, *Anal. Chem*., 2014, **86**, 6797−6803.

70 S. Kumar and P. De, *Polymer*, 2014, **55**, 824−832.

71 J. Moraes, R. Peltier, G. Gody, M. Blum, S. Recalcati, H.-A. Klok and S. Perrier, *ACS Macro Lett.*, 2016, **5**, 1416−1420.

72 V. Hildebrand, A. Laschewsky and E. Wischerhoff, *Polym. Chem*., 2016, **7**, 731–740.

73 D. Jiang, H. Zhu, W. Yang, L. Cui and J. Liu, *Sensors Actuators B*, 2017, **239**, 193–202.

74 G. R. Bardajee, M. Bayat, S. Nasri and C. Vancaeyzeele, *React. Funct. Polym.*, 2018, **133**, 45–56.

75 C. Battistella, Y. Yang, J. Chen and H.-A. Klok, *ACS Omega*, 2018, **3**, 9710−9721.

76 S. Nasri, G. R. Bardajee and M. Bayat, *Coll. Surf. B: Biointerfaces*, 2018, **171**, 544–552.

77 K. L. Heredia, G. N. Grover, L. Tao and H. D. Maynard, *Macromolecules*, 2009, **42**, 2360–2367.

78 M. Li, P. De, H. Li and B. S. Sumerlin, *Polym. Chem*., 2010, **1**, 854–859.

79 T. J. V. Prazeres, M. Beija, M.-T. Charreyre, J. P. S. Farinha and J. M. G. Martinho, *Polymer*, 2010, **51**, 355–367.

80 M. Beija, A. Fedorov, M.-T. Charreyre and J. M. G. Martinho, *J. Phys. Chem. B*, 2010, **114**, 9977–9986.

81 T. J. V. Prazeres, M. Beija, F. V. Fernandes, P. G. A. Marcelino, J. P. S. Farinha and J. M. G. Martinho, *Inorg. Chim. Acta*, 2012, **381**, 181–187.

TOC graphic

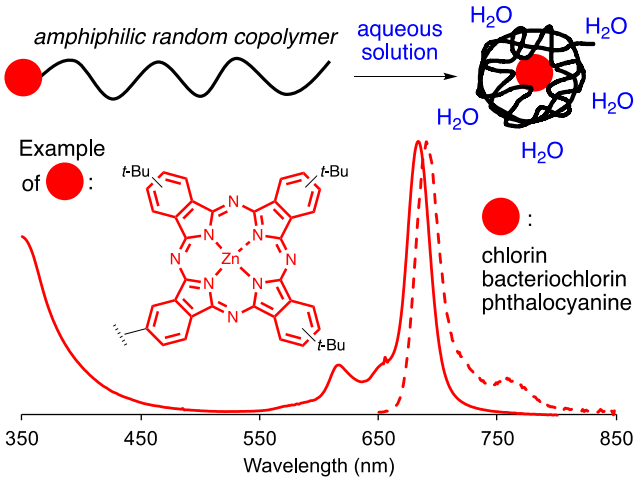

Snapping a heterotelechelic amphiphilic polymer onto a tetrapyrrole imparts aqueous solubility to the otherwise hydrophobic macrocycle as demonstrated for a chlorin, bacteriochlorin and phthalocyanine.